Magnetic Disk Drive Technology

Heads, Media, Channel, Interfaces, and Integration

Kanu G. Ashar

With contributions by
Roger F. Hoyt
Kenneth E. Johnson
James C. Suits

IEEE PRESS

IEEE Magnetics Society, *Sponsor*

The Institute of Electrical and Electronics Engineers, Inc., New York

This book may be purchased at a discount from the
publisher when ordered in bulk quantities. Contact:

IEEE PRESS Marketing
Attn: Special Sales
445 Hoes Lane, P.O. Box 1331
Piscataway, NJ 08855-1331
Fax: (732) 981-9334

For more information about IEEE Press products,
visit the IEEE Home Page: http://www.ieee.org/

10 9 8 7 6 5 4

ISBN 0-7803-1083-7

IEEE Order Number: PC4374

Library of Congress Cataloging-in-Publication Data

Ashar, Kanu G. (date)
Magnetic disk drive technology : heads, media, channel, interfaces, and integration / Kanu G. Ashar.
p. cm.
Includes bibliographical references and index.
ISBN 0-7803-1083-7
1. Data disk drives. I. Title
TK7887.8.D37A83 1996
621.39'76–dc20 96-14428
CIP

Contents

Contents

Contents

3

Disk Drive Magnetic Recording

3.1 INTRODUCTION

Multitrack magnetic audio recording in cassette and open-reel form is universally well known. The drawback of this form of recording is a long access time to a selected section on the tape. In the past, phonograph recording and, now, compact discs are preferred for quick access to a desired selection. In the 1950s, digital magnetic tapes predominated in providing on-line data storage although, for a few years in the late 1950s, expensive and complex drums were employed for critical applications requiring fast access to the data. For reasons analogous to those for the audio recording—that is, access to random data—the evolution of the rigid disk drive began in 1956. In a sense, the disk drive is a hybrid of a digital tape recorder and a phonograph jukebox. Figure 3.1 shows the parts of a disk drive. The disk is often referred to as a *platter.* Disk drive parts and their functions are given in the list that follows.

- The purpose of the disk drive is to store data over a long period of time and retrieve it reliably.
- The head writes and reads data from the disk.
- The head is part of a slider. A slider has a flexible connection to the actuator and it has a profiled surface facing the medium that forms an air-bearing surface (ABS) allowing the head to "fly" at a close distance from the medium.
- An actuator provides a means of moving the head/slider from one track to another and produces motions to retain the head in the center of the track under servo electronics commands.

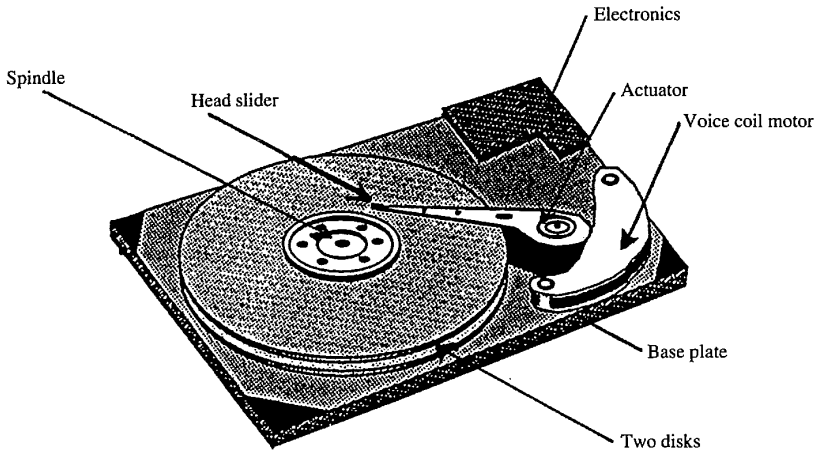

Figure 3.1 Schematic drawing of a disk drive and its parts.

- A channel converts the digital data to be stored into write currents and supplies them to the head coil. It receives signals read by the head from the medium and translates them to data or usable bit patterns.

For disk drives equal to or larger than 130 mm (5.25 in.) in diameter, linear actuators with comblike head accessing arrangements have been used. For disk diameters of 95 mm (3.5 in.) and smaller, rotary actuators are utilized. Figure 3.1 shows a rotary actuator. To shorten the latency or time of accessing on a given track, the drive rotates between 1800 and 7200 revolutions per minute (RPM). The relative velocity between head and disk is in tens of meters per second. For instance, for a 76 mm diameter track of a disk rotating at 7200 RPM, relative velocity between head and disk is about 29 m/sec (64 mi/hr). To ensure sufficiently long life for the head and magnetic medium on the disk, the head slider attached to the actuator aerodynamically "flies" at close distance of less than 100 nm (4 microinches).

After reviewing the principles of writing and reading, we shall focus on the magnetic writing of data by the head on the medium (magnetic thin layer on a substrate). The magnetic writing process is strongly tied to the recording performance of the disk drive system. Because of its importance, the discussion on writing is divided into parts. The beginning part is simple and fairly intuitive, yet it points out the limitations of the head and medium components, which has led to the evolution of recording technology. Additional topics on writing are described in the last two sections of the chapter. These issues are important for the comprehensive understanding of disk drive recording. The middle sections are dedicated to the reading processes. The significant aspects of reading are how the signal voltages and signal pulse widths vary with the head and medium parameters and the spacing between head and medium. The principles and procedures used in deriving useful equations are explained. As much as possible, simple equations are used for illustrations and clarification of concepts. More complex equations are not derived here, but their

applications and simplifications are reviewed and references are pointed out where more details can be found. An inductive head is assumed for most of the discussion. Where appropriate, the comparison of inductive and MR heads is considered, but details of the MR signal characteristics are treated in Chapter 6.

3.2 WRITING AND READING

First, we shall review the writing and reading processes. Figure 3.2 shows a schematic of a ring head and a disk. The head consists of a ring or yoke of magnetic material with a coil of wire wrapped on the core. The coil is connected to the channel electronics. There is a gap at the bottom of the head, close to the medium. The writing sequence is as follows:

1. The channel receives data to be stored from the computer, and after some processing (explained in Chapter 8), generates currents in circuits called *write drivers.*
2. The write driver supplies current to the head coil.
3. The coil current results in magnetization of the "core" of the head. Near the gap, the magnetic field spreads out.
4. Some of the fringe or stray field near the gap reaches the medium and magnetizes it in one direction as seen in Figure 3.2.

As the data changes, depending on the coding rules, the current in the coil is reversed, and the field near the gap reverses, reversing the magnetic poles in the medium. The sequence of data from the channel electronics thus gets translated into magnetized poles in the medium. During reading, the write drivers are switched off and are virtually isolated from the head coil. The reading preamplifier is connected to the head. Assuming that the disk track has previously written data, the following sequence of events or *reading* converts them into *user* bits.

1. As the magnetic poles pass near the head gap, the core of the head becomes magnetized.
2. The direction of magnetization of the core will depend on the direction of the magnetization of the medium.
3. The change in magnetization in the core results in a voltage across the head coil.

Note that only a *change* in magnetization in the medium and, hence, a *change* in magnetic flux through the coil, produces a voltage. According to Faraday's law (Sec. 2.8), $V = -d\phi/dt$ or voltage is generated if the flux changes with time. This is what happens during changing of the magnetization pattern under the head gap. At transitions, where the magnetizations in the medium change, voltage outputs result. Depending on the data, there are two types of transitions possible: north poles facing north poles or south poles facing south poles. These transitions create positive- or negative-going voltage pulses in the head coil. These voltage pulses

l references are pointed out where
ssumed for most of the discussion.
and MR heads is considered, but
ed in Chapter 6.

ıg processes. Figure 3.2 shows a
consists of a ring or yoke of mag-
e core. The coil is connected to the
n of the head, close to the medium.

from the computer, and after some
generates currents in circuits called

e head coil.
ion of the "core" of the head. Near
t.
ır the gap reaches the medium and
in Figure 3.2.

g rules, the current in the coil is re-
reversing the magnetic poles in the
el electronics thus gets translated into
ng, the write drivers are switched off
he reading preamplifier is connected
previously written data, the following
into *user* bits.

ead gap, the core of the head becomes

e core will depend on the direction of

ore results in a voltage across the head

the medium and, hence, a *change* in
voltage. According to Faraday's law
ıted if the flux changes with time. This
gnetization pattern under the head gap.
ı the medium change, voltage outputs
vo types of transitions possible: north
ıg south poles. These transitions create
in the head coil. These voltage pulses

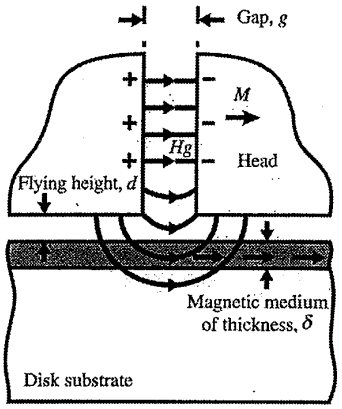

Figure 3.2 Head gap region and head fields.

get amplified and, after a series of detection steps (discussed in Chapter 8), result in usable data supplied to the computing processor.

Figure 3.3 illustrates write and read sequences. Figure 3.3a shows a sequence of data in the form of a series of "ones" and "zeros." In one method of storing this sequence of data, the current through the head coil must reverse at each "one" and not reverse at each "zero" (Fig. 3.3b). When this is done during disk rotation, the magnetization of the disk medium along a disk track looks as in Figure 3.3c. A magnetic transition occurs at each "one" and not at each "zero."

Let's turn now from *writing* data to *reading* data. The operation occurs in reverse. As a written transition passes under the head, a small change in the yoke magnetization occurs (Fig. 3.3d). This change in yoke magnetization induces a voltage in the coil that is sensed by the disk drive electronics (Fig. 3.3e). This occurs each time a transition passes under the head.

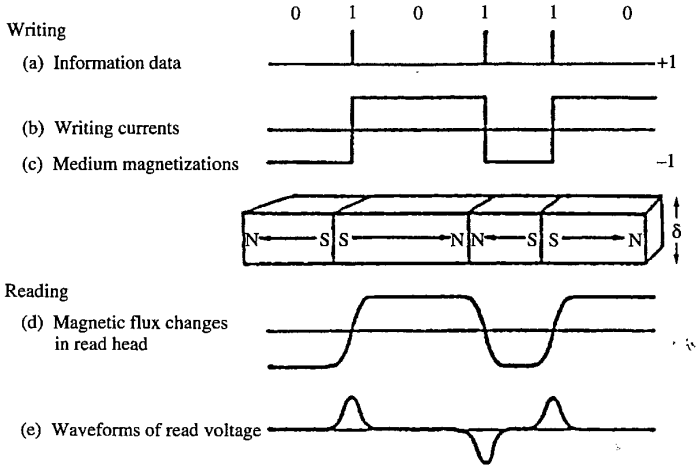

Figure 3.3 Writing and reading data.

From an energy standpoint, the writing and reading of information in the disk drive is highly inefficient. For writing, one needs currents—on the order of a few tens of milliamperes—so that the writing field at the disk medium is high enough to write. On the other hand, for reading, one only has voltages in the range 0.1 to 1 millivolts, and this requires complex external detection and amplification to extract usable data out of such low signals. However, the merit of this technology lies in its ability to store data indefinitely without power, and retrieve it inexpensively and reliably.

3.3 FIELD FROM THE HEAD

The preceding discussion gave a qualitative picture of how data are written to and read from a disk. However, to understand general design principles as well as recent improvements in head and disk designs, one needs to have a quantitative understanding of the factors involved in the writing and reading processes.

A sufficient writing field must be applied to the disk medium to write magnetic transitions. More specifically, the field produced by the head at the medium must at least exceed the coercivity of the medium. However, applying a field equal to H_c to a typical medium as shown in Figure 2.13 will reverse only half the magnetization. Due to the nonsquare nature of these loops, a field equal to two or three times H_c is applied to reverse all the magnetization. A factor of 2.5 is commonly used and will be used in illustrative examples. The stray magnetic field near the gap of an inductive head looks like that shown in Figure 3.4. This figure gives a more detailed (and inverted) picture of the head stray field previously illustrated in Figure 3.2.

The arrows indicate field direction with the length representing the magnitude of the field strength. Notice that arrow directions are effectively horizontal at the

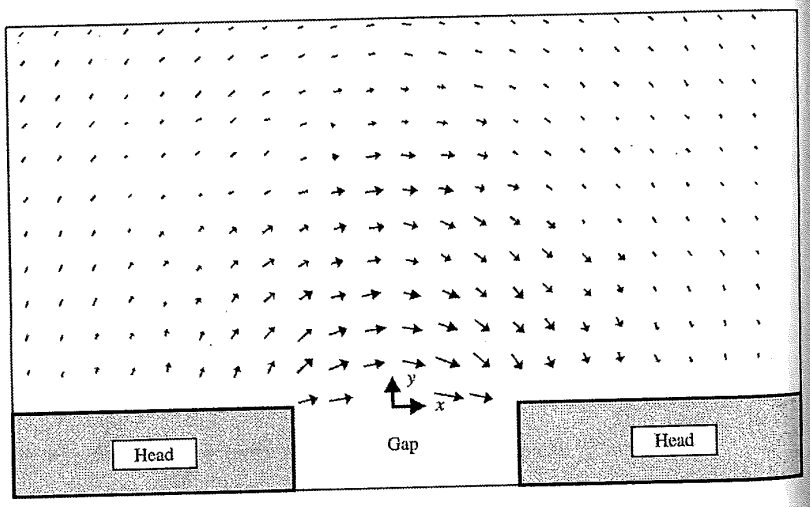

Figure 3.4 Head field and contours of equal fields.

ing of information in the disk drive
ents—on the order of a few tens of
ik medium is high enough to write.
ages in the range 0.1 to 1 millivolts,
amplification to extract usable data
this technology lies in its ability to
ve it inexpensively and reliably.

cture of how data are written to and
eral design principles as well as re-
one needs to have a quantitative un-
ng and reading processes.
to the disk medium to write magnetic
d by the head at the medium must at
vever, applying a field equal to H_c to
reverse only half the magnetization.
field equal to two or three times H_c
factor of 2.5 is commonly used and
ay magnetic field near the gap of an
3.4. This figure gives a more detailed
previously illustrated in Figure 3.2.
he length representing the magnitude
tions are effectively horizontal at the

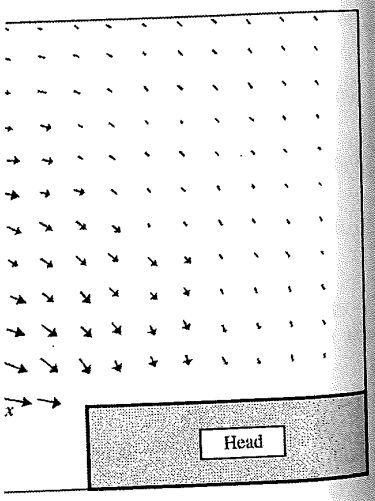

contours of equal fields.

center of the gap above the gap center. Everywhere else, they are at various angles with respect to the horizontal or x axis. First, we obtain a simple equation of the head field based on an intuitive argument and later we discuss a more accurate one. In Figure 3.4, it seems that the field contours are circular; that is, equal fields are located on the circumference of a circle. Recalling Ampere's law (refer to Sec. 2.7), the magnetic field surrounding a straight conductor with current is radially distributed, and the field is given by $I/2\pi r$, where r is the radius of the circular path. In the limiting case for the head where the gap becomes very small, the field contours become circular and the value of the field at radius r approaches $ni/\pi r$ amperes/meter. Here, i is the current in the coil, n is the number of coil turns, and ni is the ampere turns or approximately the magnetomotive force at the gap. The denominator has πr instead of $2\pi r$ because the field is integrated over a semicircle instead of a full circle as is done in the definition of Ampere's law (refer to Sec. 2.7). For longitudinal recording, our main interest is the magnetic field in the x direction. Converting the foregoing field from cylindrical (r, θ) coordinates to cartesian (x, y) coordinates, x and y components of the field are given by

$$H_x = \frac{ni}{\pi}\frac{y}{(x^2 + y^2)}, \qquad H_y = \frac{ni}{\pi}\frac{x}{(x^2 + y^2)} \tag{3.1}$$

The x field equation will be used several times in the text since it allows usable voltage signal equations and simplifies the understanding of recording concepts. Strictly speaking, the validity of the equation requires that the gap is negligible or very small compared to the distance y. In many cases, the equation is usable even when y is only slightly larger than gap g. However, as relatively smaller flying heights are used, there is a need for an accurate field equation including gap parameter for design.

More general equations for the x and y fields of a ring head of infinite poles have been derived [1] and are

$$H_x(x, y) = \frac{H_g}{\pi}\left(\arctan\frac{x + g/2}{y} - \arctan\frac{x - g/2}{y}\right) \tag{3.2}$$

$$H_y(x, y) = \frac{-H_g}{2\pi}\ln\left[\frac{(x + g/2)^2 + y^2}{(x - g/2)^2 + y^2}\right] \tag{3.3}$$

In these equations g is the gap and H_g is the magnetic field strength inside the head gap due to current in the coil (Fig. 3.2). The units of H_x and H_y are the same as the units of H_g. Since equation (3.2) plays a major role in longitudinal recording, let us examine it more closely. There is a simple way of visualizing equation (3.2). The difference of the two arctangent functions in the parentheses is nothing more than the angle θ subtended by the gap at a location x, y, where the value of field is required. The geometric construction is illustrated in Figure 3.5.
Accordingly, equation (3.2) can be simply written as

$$H_x(x, y) = \frac{H_g}{\pi}\theta \tag{3.4}$$

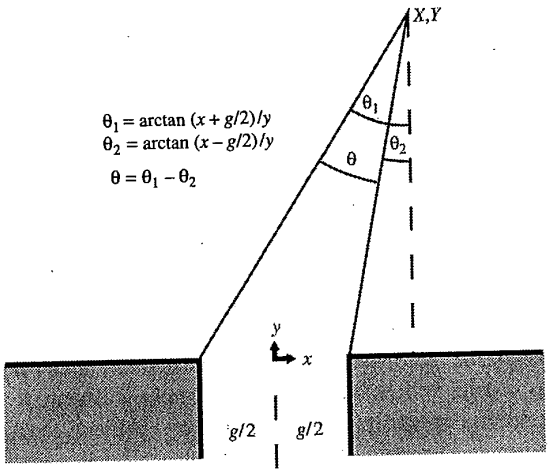

Figure 3.5 Karlqvist head field in terms of an angle.

where θ is as defined in the last paragraph and is in radians. $H_x(x, y)$ is the largest where θ is the largest; that is, from Figure 3.5 where the point of interest x, y is closest to the gap and directly over the gap ($\theta = \pi$ and $H_x = H_g$). Using the angle θ, one can qualitatively plot the contours of equal fields surrounding the gap of a ring head.

Figure 3.6 shows plots of H_x and H_y along the x and y axes. The x-axis values are divided by g, and head fields H_x and H_y are divided by H_g to make these uni-

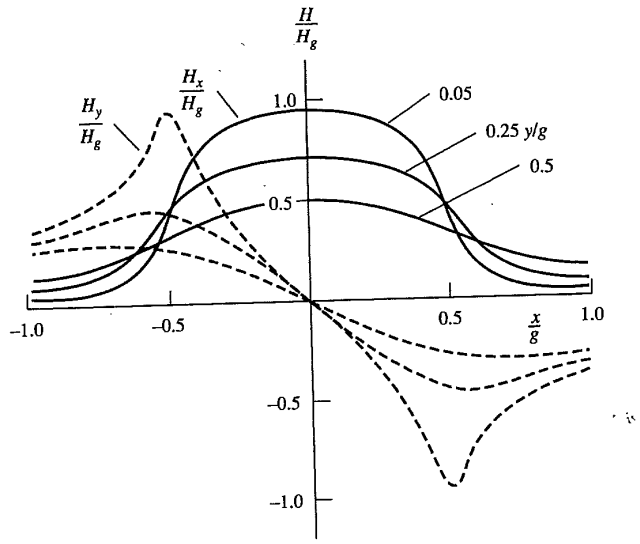

Figure 3.6 Normalized x and y components of head field.

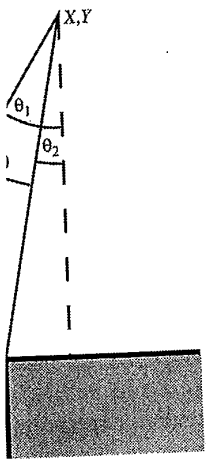

n terms of an angle.

is in radians. $H_x(x, y)$ is the largest
5 where the point of interest x, y is
$= \pi$ and $H_x = H_g$). Using the angle
qual fields surrounding the gap of a

ng the x and y axes. The x-axis val-
are divided by H_g to make these uni-

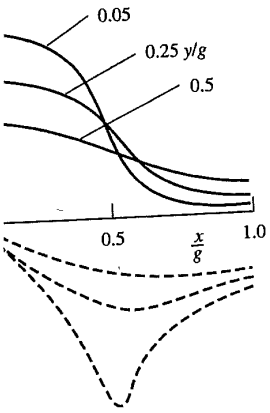

components of head field.

versal plots, that is, independent of particular g and H_g values. Three field contours are shown for y/g values of 0.05, 0.25, and 0.5. As illustrated earlier in Figure 3.4, the H_x component of the field (solid lines in Fig. 3.6) is maximum along the vertical axis. H_x also is shown growing larger as y becomes smaller, that is, nearer the head. H_y, on the other hand (dashed lines), is zero at the gap center; there is no vertical component of the field along the vertical center line (see Fig. 3.4). However, this field peaks at some distance from the center line. It turns out that the locations on the x axis, where the H_y field is a maximum or a minimum in Figure 3.6, are the points where the H_x field is 50% of the maximum value of H_x. The values of x, where H_y has a maximum and a minimum, are obtained by differentiating it with respect to x on the right-hand side of equation (3.2) and equating the result to zero. We define the distance between these two x values, where H_x is 50% of its peak value as the half width (Δx) of H_x. The value of Δx can be obtained in equation form by manipulating equations (3.2) and (3.3).

$$\Delta x = 2\left[\left(\frac{g}{2}\right)^2 + y^2\right]^{1/2} \tag{3.5}$$

The equation gives the half width of the x component of the head field. In Section 3.7, it will be seen that under certain conditions, the shape of the read voltage pulse becomes identical to that of the head field, and the same equation (3.5) gives a pulse half width of the read voltage. Note that in the close vicinity of the gap ($y = 0$), Δx becomes equal to the gap size g. Putting $x = 0$ in equation (3.2), we get the (peak) horizontal field along the y axis. This equation is plotted in Figure 3.7.

$$H_x(0, y) = \frac{2H_g}{\pi} \arctan \frac{g}{2y} \tag{3.6}$$

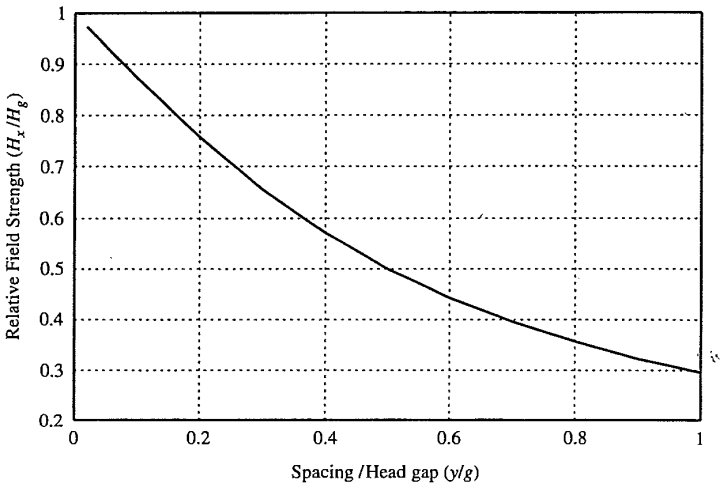

Figure 3.7 Peak head field as a function of the ratio of spacing and gap.

The following example is given to demonstrate the use of this equation and increase familiarity with the nomenclature. The example also points out the importance of parameters that lead to head and medium technology enhancements.

3.4 EXAMPLE: HEAD FIELD CALCULATION

The objectives are, first, to calculate the head gap field, which allows writing magnetic transitions on the medium and second, to calculate the current required in the head coil to produce this field. The following parameters are assumed:

1. The medium has a coercivity of 1600 Oe (127 kA/m).
2. A field H_x equal to 2.5 times the coercivity of the medium is required for proper writing.
3. Head gap $g = 400$ nm.
4. Flying height (magnetic distance between head and medium, Fig. 3.2) $y = 100$ nm.
5. Medium thickness is considered negligibly small compared to the flying height.

Solving equation (3.6) for H_g results in $H_g = 5666$ Oe (451 kA/m).

More easily and less accurately, Figure 3.7 may be used to calculate the same quantity. For $y/g = 100$ nm/400 nm $= 0.25$, $H_x/H_g = 0.7$. For a field at the medium of 1600 Oe (127 kA/m) $\times$ 2.5 $=$ 4000 Oe (318 kA/m), a gap field of 4000 Oe/0.7 $=$ 5700 Oe (454 kA/m) is required.

This field in the gap is generated by the head coil current. It is assumed that all the ampere turns (current multiplied by number of turns) are utilized to produce a head gap field. This happens if the permeability of the head material is very high. The magnetomotive force (refer to Sec. 2.10) required to produce a gap field is given by $H_g \times g = (451 \times 10^3) \times (400 \times 10^{-9}) = 180.4$ ma for a single-turn head. For a 20-turn head a current of 9 ma would be required. In practice, the permeability of the material is finite, and not all the field generated by the coil reaches the head gap. To account for the geometry of the head and permeability of the head core, the term "head efficiency" is introduced. The next section describes a formula to calculate head efficiency for a ring head structure.

3.5 HEAD EFFICIENCY AND FIELD IN THE GAP

The magnetic circuit of the ring head can be approximated by two reluctances in series: that of the head gap and that of the head core (see Sec. 2.10 for a discussion of magnetic circuits). These reluctances are given by $\mathcal{R}_g$ and $\mathcal{R}_c$ as

$$\mathcal{R}_g = \frac{g}{\mu_0 A_g}, \qquad \mathcal{R}_c = \frac{l_c}{\mu A_c} \tag{3.7}$$

where g and l_c = the lengths of the gap and head core
A_g and A_c = the gap and head core areas, respectively
μ = the permeability of the head core material.

3.6 RE

se of this equation and increase
so points out the importance of
y enhancements.

eld, which allows writing mag-
ulate the current required in the
neters are assumed:
(127 kA/m).
ty of the medium is required for

head and medium, Fig. 3.2) y =

ly small compared to the flying

66 Oe (451 kA/m).
nay be used to calculate the same
$H_x/H_g = 0.7$. For a field at the
) Oe (318 kA/m), a gap field of

ad coil current. It is assumed that
er of turns) are utilized to produce
of the head material is very high.
ired to produce a gap field is given
30.4 ma for a single-turn head. For
ed. In practice, the permeability of
d by the coil reaches the head gap.
neability of the head core, the term
n describes a formula to calculate

P

pproximated by two reluctances in
core (see Sec. 2.10 for a discussion
en by $\mathcal{R}_g$ and $\mathcal{R}_c$ as

$$_c = \frac{l_c}{\mu A_c} \tag{3.7}$$

the gap and head core
ad core areas, respectively
ty of the head core material.

The magnetomotive force provided by the coil current is divided between these two reluctances. Since the magnetomotive force (mmf) across the gap results only in a gap field, the efficiency of the head is given by

$$\eta = \frac{\mathcal{R}_g}{\mathcal{R}_g + \mathcal{R}_c} = \frac{1}{1 + (l_c\mu_0/g\mu)(A_g/A_c)} \tag{3.8}$$

The total mmf is the ampere turns ni which is the summation of mmfs across the head core and the gap; that is, $ni = H_g\, g + H_h\, l_c$. Hence, efficiency in terms of ampere turns or mmf is defined as

$$\eta = \frac{H_g g}{H_h l_c + H_g g} = \frac{H_g g}{ni} \tag{3.9}$$

Solving equation (3.9) for H_g gives

$$H_g = \eta \frac{ni}{g} \tag{3.10}$$

Substituting equation (3.8) into (3.10) gives

$$H_g = \frac{ni}{g + (l_c\mu_0/\mu)(A_g/A_c)} \tag{3.11}$$

Equation (3.11) is the final equation, giving the head gap field in terms of the geometry of the head (n, g, l_c, A_g, A_c), head material (μ), and current (i) through the head coil. Substituting this into equations (3.2) and (3.3) allows us to calculate the head field at a given location x, y near the head gap.

Equation (3.10) has a limitation. Increasing the current in a ring head coil does not increase H_g indefinitely. Once the magnetization of the yoke reaches its saturation value M_s, no additional field may be created on the gap surface and the H_g attains its maximum value, which turns out to be M_s. The highest value of saturation magnetization M_s for ferrite material is obtained in hot-pressed MnZn ferrite and is about 6000 gauss (480 kA/m); hence, this is the maximum value of H_g. This points out a limitation of ferrite heads and suggests a motivation for the development of metal-in-gap (MIG) and thin film heads.

3.6 READING OF MAGNETIC DISK DATA

Writing and reading processes are qualitatively discussed in Section 3.2. The next few sections describe reading in more detail. When a magnetic transition on the disk medium (Fig. 3.3c) passes under the ring head, a voltage is induced in the coil of the head (Fig. 3.3e). This voltage constitutes the read signal from the disk. The objective now is to formulate equations for this induced voltage as a function of head parameters, media parameters, and flying height. These equations are used by the designer to arrive at appropriate compromises in selecting components and channel electronics. Some of these results point out the evolution of new technological developments toward high-density disk drive recording.

Sections 3.3, 3.4, and 3.5 discussed the head field as a function of head geometry and current through the coil. In this section, a voltage equation is derived by relating the head field to the medium magnetization. In this discussion, only the x component of the field and medium magnetizations are considered; hence, the subscript y is omitted in their representations. The longitudinal head field $H(x)$ creates a magnetic flux $\phi_m(x)$ in the media

$$\phi_m(x) = \mu_0 H(x) w \delta \tag{3.12}$$

where w is the track width and δ is the medium thickness. The current in the head coil generates the magnetic field, and it magnetizes the medium. For reading, it is useful to formulate how the magnetized transitions in the medium result in flux changes in the head coil, which in turn produces an output signal. Every element of the magnetized medium contributes to flux change in the head gap and generation of voltage pulse. If contributions of all the elements of the medium are integrated, total flux changes and output voltage pulse can be obtained. However, this procedure is difficult to carry out analytically. There is a shortcut method known as the *principle of reciprocity,* which simplifies the mathematical derivation. Those familiar with the concept of mutual inductance between two coils already know the reciprocity principle. Figure 3.8 shows two coils, one of the head and the other (virtual coil) of medium magnetization. When current i_h flows through the head coil, flux ϕ_m is generated in the section of the medium and is given by

$$\phi_m = L_{hm} i_h \tag{3.13}$$

where L_{hm} is the mutual inductance between two coils.

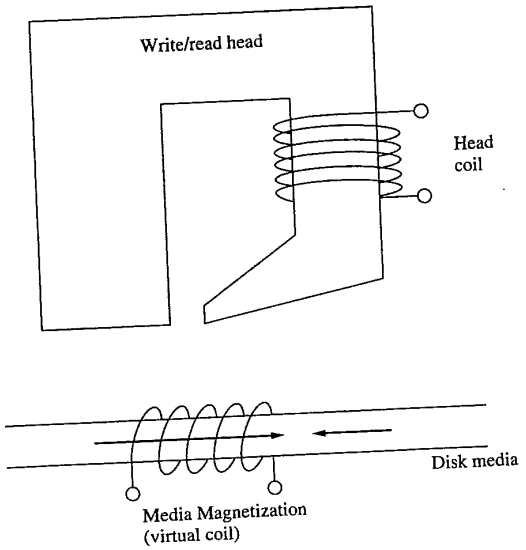

Figure 3.8 Principle of reciprocity applied to head and magnetic media.

d field as a function of head geom-
ı, a voltage equation is derived by
ıtion. In this discussion, only the x
ɔns are considered; hence, the sub-
ongitudinal head field $H(x)$ creates

$)w\delta$ (3.12)

thickness. The current in the head
etizes the medium. For reading, it
sitions in the medium result in flux
; an output signal. Every element of
ge in the head gap and generation of
s of the medium are integrated, total
btained. However, this procedure is
:tcut method known as the *principle*
cal derivation. Those familiar with
) coils already know the reciprocity
he head and the other (virtual coil)
ws through the head coil, flux ϕ_m is
given by

h (3.13)

wo coils.

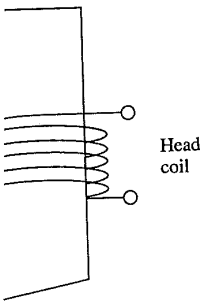

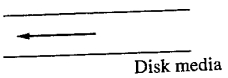

n

ied to head and magnetic media.

Likewise, under the influence of medium magnetization (virtual current), flux ϕ_h is generated in the head coil and is given by

$$\phi_h = L_{mh} i_m \tag{3.14}$$

The reciprocity principle simply states that these mutual inductances are equal. With this consideration, flux in the head coil due to medium magnetization is given as

$$\phi_h = i_m \frac{\phi_m}{i_h} \tag{3.15}$$

Now at any point in the medium, the track is rotating at a velocity v; hence, location of a point in medium with reference to center line of the head ($x = 0$) is given by $x - x'$, where x' is equal to vt. Medium magnetization at a point is given by $M(x - x')$. This magnetization along the length of distance dx for an area of $w\delta$, where δ is the medium thickness and w is the track width, can be treated as a source of current with magnitude:

$$i_m = M(x - x')dx \tag{3.16}$$

Combining equations (3.15), (3.16), and (3.12), the head field due to an element of medium magnetization is given by

$$d\phi_h = \mu_0 w\delta M(x - x')dx \frac{H(x)}{i_h} \tag{3.17}$$

The total field in the head coil due to medium magnetization is given by the integration

$$\phi_h(x') = w\delta\mu_o \int_{-\infty}^{\infty} M(x - x') \frac{H(x)}{i_h} dx \tag{3.18}$$

The reciprocity relation utilized in the preceding derivation is a basic technique frequently used in magnetic recording; hence, we give here a slightly modified example from [2] that illustrates the principle of reciprocity very well. Interference from a local FM station at a frequency range in excess of 88 MHz is often experienced by engineers during tests on test stands. The noise of several microvolts in the head output signal from such a source is observed if the room is poorly shielded. Let us say that a 100-ampere current in a station antenna creates 10 μV of noise in the head under test. If we were to pass a 100-ampere current through the head (not practical!), the radio station would experience 10 μV of noise on its signal. If we know the result of transmission in one direction, the outcome for the reverse condition can be predicted.

Equation (3.18) is often stated as a three-dimensional integral [4]. However, in practice, medium magnetization in the x direction is the most important one. Assumption of uniform magnetization along the z direction results in track width w in the equation, and summation of fields in the y direction results in the medium thickness δ. It is also implied that the head to medium spacing d is large compared

to medium thickness δ. The next step is to obtain the voltage equation as a function of t or x', which is vt, where v is the velocity of disk rotation:

$$V(x') = V(vt) = -n\frac{d\phi}{dx'}\frac{dx'}{dt} = -nv\frac{d\phi}{dx'} \tag{3.19}$$

Note that n is the number of head turns. Combining equations (3.18) and (3.19), we obtain

$$V(x') = -\mu_o nvw\delta \int_{-\infty}^{\infty} \frac{dM(x-x')}{dx'}\frac{H(x)}{i_h}dx \tag{3.20}$$

For an explicit analytical function of the voltage, it is necessary to define the slope of medium magnetization within the transition. For a qualitative look at voltage generation as a result of medium transitions, see Figure 3.3.

3.7 READING WITH STEP-FUNCTION MAGNETIC TRANSITIONS

In equation (3.20), the voltage of a ring head is expressed as a function of the derivative of medium magnetization. This derivative can be evaluated if the magnetization and its changes in the x direction are known. Magnetization and its transitions in magnetic recording are widely studied subjects and are reported in many textbooks and papers. Three types of transitions have been studied in detail:

1. An ideal step-function transition (Fig. 3.9).
2. A transition with magnetization in the transition region obeying an arctan function of distance (Fig. 3.10).
3. Transitions with magnetization varying as a sinusoidal function in the x direction (Fig. 3.18).

First, assume that the magnetization change or transition is a step function, that is, the magnetization in the transition, M_x, that goes abruptly from $-M_r$ to $+M_r$ at location $x = x'$ (Fig. 3.9), where M_r is the remanent magnetization of the medium. The derivative of a step function is known as a *Dirac delta function* and is designated by δ (we will call it δ_D to distinguish it from our medium thickness). Differentiation of M_x will be given by

$$\frac{dM_x(x-x')}{dx} = 2M_r\delta_D(x-x') \tag{3.21}$$

By substituting equation (3.21) into equation (3.20) and using the standard property of integrals involving the delta function, equation (3.20) becomes

$$V(x') = -2\mu_o nvw(M_r\delta)\frac{H(x')}{i_h} \tag{3.22}$$

the voltage equation as a function
lisk rotation:

$$\frac{c'}{t} = -nv\frac{d\phi}{dx'} \tag{3.19}$$

ng equations (3.18) and (3.19), we

$$\frac{x - x')}{dx'}\frac{H(x)}{i_h}dx \tag{3.20}$$

, it is necessary to define the slope
. For a qualitative look at voltage
Figure 3.3.

xpressed as a function of the deriva-
an be evaluated if the magnetization
Magnetization and its transitions in
and are reported in many textbooks
n studied in detail:

3.9).
transition region obeying an arctan

ng as a sinusoidal function in the

nge or transition is a step function
f_x, that goes abruptly from $-M_r$ t
is the remanent magnetization of the
known as a *Dirac delta function* an
guish it from our medium thickness

$$_r\delta_D(x - x') \tag{3.21}$$

3.20) and using the standard proper
ition (3.20) becomes

$$(M_r\delta)\frac{H(x')}{i_h} \tag{3.22}$$

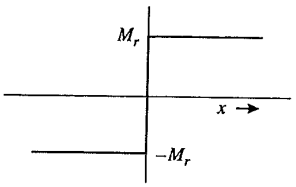

Figure 3.9 Step-function transition of medium magnetization.

This equation suggests a number of important points.

1. The voltage output of an inductive head is directly proportional to $H(x')$. Because of this proportionality, measurement of the voltage pulse waveform reflects the head field characteristics. This could be used to characterize head geometry.
2. The voltage is proportional to $M_r\delta$, which contains all the medium parameters. This quantity indicates medium *strength*. For example, in the case of a particulate medium, the particles of the magnetic material are relatively far apart and have low magnetization; hence, it is difficult to obtain a high M_r. For thin magnetic coatings, 100% of the medium material is magnetic, so M_r can be quite large. The film thickness can be very small, yet the product $M_r\delta$ can be sufficiently large to give adequate signal voltage.
3. The voltage output of an inductive head is also proportional to the number of coil turns n, the velocity of the disk v, and the track width of the head w.

Until now, we have not considered the efficiency of the head, but that term also directly multiplies to the right-hand-side function of the voltage. Substitution of equations (3.2) and (3.10) in (3.22) gives analytical function of the voltage,

$$V(x') = -2\mu_o\left(\frac{\eta nvw}{\pi g}\right)(M_r\delta)\left(\arctan\frac{x' + g/2}{d} - \arctan\frac{x - g/2}{d}\right) \tag{3.23}$$

where d is the flying height (parameter y). The peak voltage can be obtained by putting $x' = 0$ in equation (3.23) and P_{50}, or the half width of the voltage pulse is the same as the half width of the field and is given by equation (3.5).

3.8 READING ARCTANGENT MAGNETIC TRANSITIONS

The most widely used assumption in digital recording about the shape of the magnetization is an arctan function of x [3]. This is given as

$$M_x = \frac{2}{\pi}M_r\left(\arctan\frac{x}{a}\right) \tag{3.24}$$

At large values of $+x$ and $-x$, the arctan function approaches $+\pi/2$ and $-\pi/2$, respectively, making M_r and $-M_r$ limiting values for M_x (Fig. 3.10). Only one

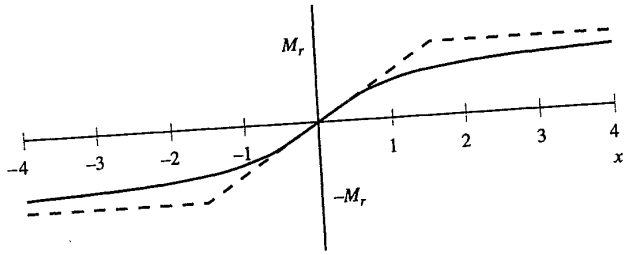

Figure 3.10 Arctan magnetic transition.

parameter a is needed to specify the transition characteristics. The parameter a is known as the *transition parameter* and is a measure of the width of the transition. The voltage equation is obtained by substituting arctan function for the magnetization transition in equation (3.20) and integrating. We shall not go into this process but simply give the result.

$$V(x',d) = -2\mu_0\left(\frac{\eta n v w}{\pi g}\right)(M_r\delta)\left(\arctan\frac{x' + g/2}{a+d} - \arctan\frac{x' - g/2}{a+d}\right) \tag{3.25}$$

This equation has the same form as that of equation (3.23), except that in place of d, $a + d$ is substituted. This is interesting and important, as the effect of transition broadening from width 0 (step function) to width a is equivalent to adding a to flying height d, making effective flying height as $a + d$. Substituting $x' = 0$ in equation (3.25), the peak voltage for this case is obtained,

$$V_{p-p} = 8\mu_0\left(\frac{\eta n v w}{\pi g}\right)(M_r\delta)\arctan\left(\frac{g/2}{a+d}\right) \tag{3.26}$$

and substituting $a + d$ in place of y in equation (3.5), the half width of the voltage pulse is given by

$$P_{50} = 2\left[\left(\frac{g}{2}\right)^2 + (a+d)^2\right]^{1/2} \tag{3.27}$$

Note that a and d in equations (3.26) and (3.27) always occur as a summation $a + d$. Decreasing $a + d$ increases peak voltage and reduces the half width of the voltage pulse or slims the pulse. Narrow pulses allow increased linear density. Much research is directed toward (1) decreasing d by innovations in the head-disk interface and (2) improving medium to achieve shorter a. Sections 3.11 and 3.12 discuss plots of these parameters and engineering optimization of the system using these equations. Derivation of equation (3.27) assumes that the thickness of the medium is very small compared to flying height. However, the equation can be generalized, including medium thickness, and the result is given as [4].

3.9 TRA

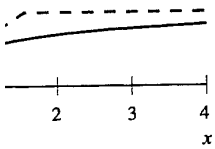

ansition.

aracteristics. The parameter a is
e of the width of the transition.
ctan function for the magnetiza-
We shall not go into this process

$$- \arctan \frac{x' - g/2}{a + d}\Bigg) \tag{3.25}$$

n (3.23), except that in place of
ortant, as the effect of transition
a a is equivalent to adding a to
$a + d$. Substituting $x' = 0$ in
btained,

$$\text{ctan}\left(\frac{g/2}{a + d}\right) \tag{3.26}$$

.5), the half width of the voltage

$$d)^2\Big]^{1/2} \tag{3.27}$$

') always occur as a summation
e and reduces the half width of
es allow increased linear density.
d by innovations in the head-disk
shorter a. Sections 3.11 and 3.12
g optimization of the system us-
7) assumes that the thickness of
ht. However, the equation can be
e result is given as [4].

$$P_{50} = 2\left[\left(\frac{g}{2}\right)^2 + (a + d)(a + d + \delta)\right]^{\frac{1}{2}}$$
$$= [g^2 + 4(a + d)(a + d + \delta)]^{\frac{1}{2}} \tag{3.28}$$

3.9 TRANSITION PARAMETER a

Achieving the narrowest possible transition (smallest a value) allows placing recorded bits close together and hence results in high linear density. Until now, we have not defined how one can find this parameter. Several authors have reported the derivation of a by taking into account a detailed writing process using nonlinear B–H loop (refer to Sec. 2.13) characteristics of the medium [2–5]. The most practical equation used for head-disk modeling studies is given by

$$a = K\left(\frac{M_r \delta d_{\text{eff}}}{H_c}\right)^{1/2} \tag{3.29}$$

where $M_r\delta$ has the same meaning used in this chapter. H_c is the coercivity of the medium. In the equation, M_r and H_c are expressed in SI units (A/m). If M_r and H_c are expressed in cgs units, that is, emu/cm^3 and Oe, M_r is multiplied by 4π as ampere/meter. K is a constant derived analytically after several considerations, some of which are

1. The head field applied during writing is optimized for shortest transition distance.
2. The demagnetization field is taken into account.
3. Head imaging into the medium is included.
4. Finite remanent coercivity of the medium is also included.

The approximate value of K from [3] and [6] is 0.87. With simplifications of a Lorentzian pulse form in place of the Karlqvist field function and other assumptions [4], the value of K turns out to be $1/\sqrt{\pi}$, or 0.565. In case of cgs values for M_r and H_c, K modifies to 3.1 and 2, respectively. The d_{eff} is the geometrical mean distance from head to medium and is expressed by

$$d_{\text{eff}} = [d(d + \delta)]^{1/2} \tag{3.30}$$

Equation (3.29) indicates that the reduction in a and increased linear density may be achieved by decreasing the effective flying height d_{eff}, increasing the coercivity H_c of the medium, and decreasing the thickness δ of the magnetic medium. Smaller M_r could also reduce a, but as seen in equation (3.26), a smaller $M_r\delta$ would reduce the signal voltage, and so there must be a compromise.

Increasing the coercivity H_c of the medium requires a larger write field from the head. This has motivated the development of MIG heads, thick-pole thin-film heads, and high-magnetic-moment materials for MR-head write elements.

3.10 EXAMPLE: CALCULATIONS OF TRANSITION PARAMETER *a*, V_{p-p}, AND P_{50}

This example is chosen to put some real dimensions into the use of the preceding equations. One of the problems in making calculations of recording parameters is mixed units. We intend to use SI units as much as possible. However, some scientists and engineers are not going to abandon the use of cgs units, so one objective of this exercise is to practice conversions of popular units into SI units to arrive at useful, final results. A discussion of units will contribute to an understanding of the concepts. So clarification of ideas is yet another goal of the example. The following parameters are assumed for this exercise:

η = 0.8 efficiency of the head
n = 30 head coil turns
v = 20 meters per second, velocity of the medium under head
w = 8 μm, track width of the head
g = 0.25 μm
M_r = 800 kA/m (800 emu/cm^{-3})
δ = 30 nm (300 A°), medium thickness
d = 100 nm (4 μin.)
H_c = 130 kA/m (1600 Oe)
$\mu_0 = 4\pi \times 10^{-7}$ Vs/Am (H/m)

$M_r\delta$ in SI units is $800{,}000 \times 30 \times 10^{-9} = 24 \times 10^{-3}$ A (2.4×10^{-3} emu/cm^{-2}). Note that in SI units, medium strength is expressed in the unit of current. Treatment of medium strength as a coil current is exemplified by the unit dimension. One can express $M_r\delta$ as 24 milliamperes of current.

Next, a is calculated from equation (3.29). Since we want an answer for a in nanometers, δ and d_{eff} can be retained in nanometers for the calculation. Using the value of K as 0.87, a is computed to be 119 nm. Equation (3.26) is used for the calculation of peak-to-peak voltage V_{p-p}. $M_r\delta$ should be expressed in amperes, as shown earlier. The ratio of track width to gap need not be converted into meters and can be written in micrometers. The quantities in the ratio of gap to the summation of d and a within the arctan function can also be totally expressed in nanometers and need not be converted to meters. The V_{p-p} is calculated to be (1180 × arctan function value of 0.518) × 10^{-6} volts, or 616 μV. It is common practice to express head

quires a larger write field from
MIG heads, thick-pole thin-film
R-head write elements.

P_{50}

ns into the use of the preceding
tions of recording parameters is
ssible. However, some scientists
f cgs units, so one objective of
r units into SI units to arrive at
ribute to an understanding of the
al of the example. The following

iedium under head

10^{-3} A (2.4×10^{-3} emu/cm^{-2})
ed in the unit of current. Treatment
ed by the unit dimension. One can

Since we want an answer for a in
eters for the calculation. Using the
m. Equation (3.26) is used for the
should be expressed in amperes, as
ed not be converted into meters and
the ratio of gap to the summation of
otally expressed in nanometers and
lculated to be (1180 × arctan func
is common practice to express hea

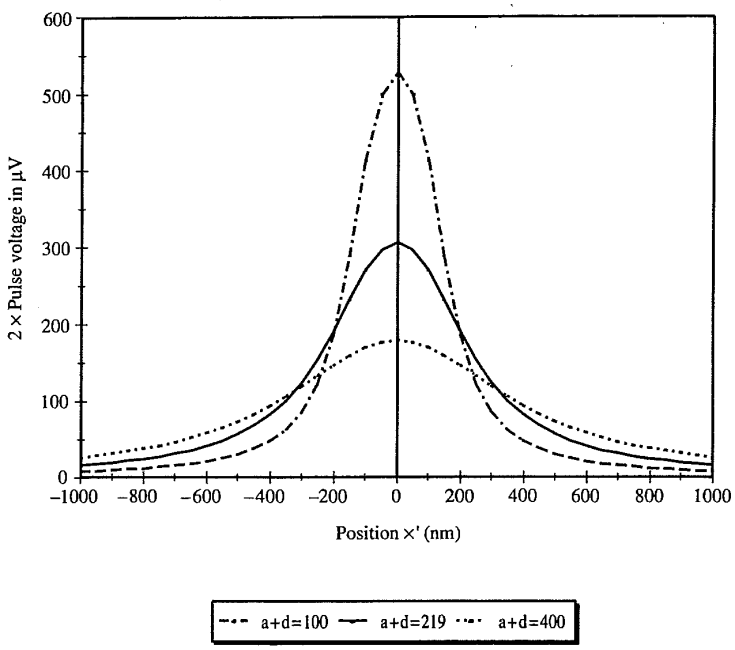

Figure 3.11 Isolated pulse voltage variations with spacing and transition parameters.

voltage in nanovolts per 1-μm track width, per meter/sec velocity, and per turn. This quantity is calculated as 127 nV/μm per m/sec per turn. This method of normalizing signal voltage is useful in comparing heads. Half-pulse width P_{50} is calculated from equation (3.28): $P_{50} = [(250)^2 + 4(119 + 100)(119 + 100 + 30)]^{1/2} = 530$ nanometers. P_{50} is an important parameter that determines the ability of the system to achieve high densities. These topics are discussed in Chapter 8, Section 8.18.

3.11 SIGNAL VOLTAGE PARAMETERS AND ENGINEERING APPROXIMATIONS

Voltage pulses described in equations (3.25) and (3.26) and half-width expressions (3.28) are now analyzed as functions of a head/disk system. The parameters used in the example in Section 3.10 are also used in plotting the graphs discussed later in this chapter. It should be noted that much of this discussion applies to inductive (ferrite, MIG, and film) heads. A similar analysis is carried out for MR heads in Section 6.18. Certain parameters like gap, g, get modified for MR head, and there is no velocity dependence for the magnetoresistive heads. Figure 3.11 shows three pulses

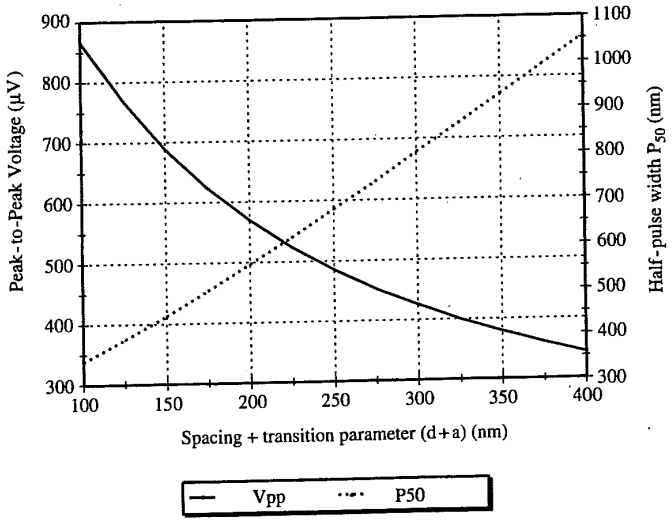

Figure 3.12 Peak-to-peak voltages and half-pulse widths versus $d + a$.

calculated using equation (3.25) with variations in parameter $d + a$. As described earlier, d is the head-medium spacing, and a is the transition parameter. In the equations these parameters always occur as a summation, so conclusions drawn from the figure are valid if only one parameter is varied at a time or both the parameters are changed simultaneously. As $a + d$ is increased, the voltage peak decreases. Also the pulse gets widened, making P_{50} larger as a function of $a + d$. This is further illustrated in Figure 3.12. In Figure 3.12, peak-to-peak voltage (equation 3.26) and P_{50} (equation 3.28) are plotted as continuous functions of $a + d$. The message is clear that low-flying heights and narrow transitions are important to get adequate signal and short-pulse widths.

The signal voltage is related to thin film medium saturation magnetization M_r in two ways. Higher M_r results in increased signal strength and hence an increase in output voltage. However, a large M_r increases the transition parameter a, which tends to reduce voltage. Figure 3.13 shows the cross-over in case of M_r versus isolated peak-to-peak signal voltage. The figure also shows the increase in P_{50} as a function of M_r because of increasing values of a.

Practitioners prefer simple expressions for quick derivations and comparisons with experimental results. Here are some ideas which may be helpful. Section 3.3 indicated that if the gap of the head is very small, an approximate $H_x(x, y)$ field is obtained as given by equation (3.1). If this approximation is used instead of the Karlqvist equation in the integration of equation (3.20), a simple voltage pulse form can be given as

$$V(x) = \frac{V_{\max}}{1 + (2x/P_{50})^2} \tag{3.31}$$

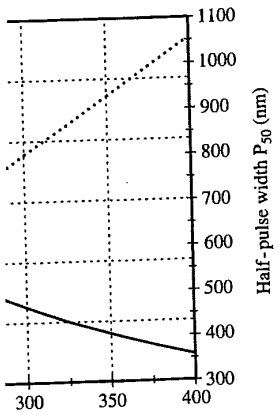

ılf-pulse widths versus $d + a$.

ıs in parameter $d + a$. As described
the transition parameter. In the equa-
ıation, so conclusions drawn from the
l at a time or both the parameters are
ed, the voltage peak decreases. Also
a function of $a + d$. This is further
-to-peak voltage (equation 3.26) and
functions of $a + d$. The message is
sitions are important to get adequate

medium saturation magnetization M_r
signal strength and hence an increase
ıses the transition parameter a, which
the cross-over in case of M_r versus
ıre also shows the increase in P_{50} as a
of a.
for quick derivations and comparisons
as which may be helpful. Section 3.
small, an approximate $H_x(x, y)$ field
s approximation is used instead of the
ion (3.20), a simple voltage pulse form

$$\frac{V_{max}}{2x/P_{50})^2} \qquad (3.31$$

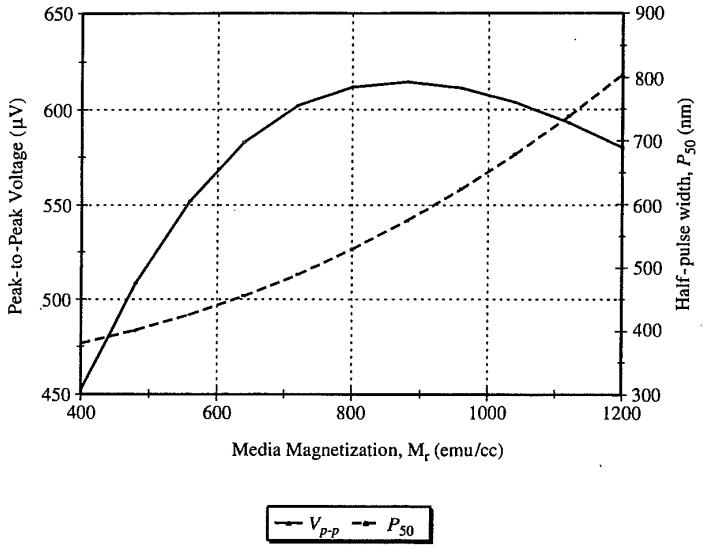

Figure 3.13 V_{p-p} and P_{50} versus media magnetization M_r.

where P_{50} is given by $a + d$. This equation is known as a *Lorentzian pulse,* and one can see that at $x = \pm P_{50}/2$, the voltage is half its peak value, which confirms the definition of P_{50}.

To verify the degree of validity and usefulness of equation (3.31), the normalized value of equation (3.25) is compared with the normalized value of equation (3.31) in Figure 3.14.

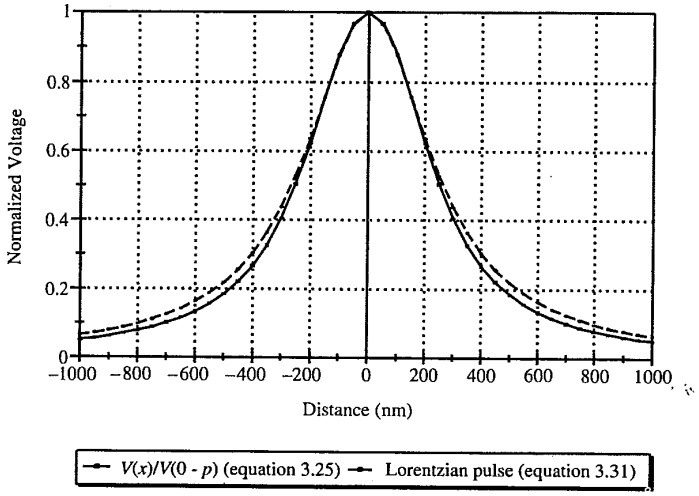

Figure 3.14 Comparison of normalized voltage waveform with Lorentzian pulse.

Normalization of equation (3.25) means that the equation is divided by zero-to-peak voltage (1/2 of peak-to-peak voltage of equation 3.26) so that the peak value of normalized voltage is 1. Normalization of equation (3.31) is obtained by dividing the right side of the equation by V_{max}. The correlation between these two cases is good. One application of this form of equation is to compute the roll-off curve to obtain resolutions of the overlapping pulses at high densities. This is described in Chapter 8.

Equation (3.31) would be more useful if there were some way of estimating V_{max}. Here we suggest an approximate procedure useful for a rough estimate. Observation of Figure 3.12 suggests reciprocal relationship between P_{50} and V_{p-p}. Utilizing this observation and information from the accurate equations described, V_{max} may be derived from

$$V_{max} \propto \frac{\mu_0 nvw(M_r\delta)}{P_{50}} \tag{3.32}$$

where all the variables are as discussed earlier. So the task boils down to finding the proportionality constant, which may be obtained experimentally.

3.12 DIGITAL WRITING PROCESS: DISCUSSION AND GRAPHICAL ILLUSTRATION

A large amount of experimental and analytical or numerical modeling has been done on the subject of the write process in magnetic recording. However, the complete solution of the process has not been attained, as it involves nonlinear and complex medium magnetization processes, transition formation details, and dynamics of head and medium interactions.

Here we shall describe only the qualitative principles of the writing procedures to understand interactions among component properties and parameters. Two parameters of interest involve how the transition of magnetization from one direction to the other is formed: what contributes to the variability in its length, and what contributes to the variation in distance (length jitter) between such transitions. The first parameter is useful in designing for high linear density, and the second pertains to error-free detection of the signal. The writing process includes application of current to the head coil, which produces a field in and near the gap of the head. The field reaching the medium either supports the existing direction of magnetization direction or opposes it, creating a reversed magnetized region in the medium. The process of medium magnetization follows the M–H (medium magnetization as a function of applied field H, see Section 2.13) hysteresis loop curve. The magnetization reversal in the medium happens in the spread-out region, and this is the transition region we referred to in the last few sections. Going through the step-by-step understanding of the writing process will help the practitioner know the measures used to design the write/read electronics as well as appreciate the measurement practices used in the industry.

equation is divided by zero-to-
ion 3.26) so that the peak value
ɔn (3.31) is obtained by dividing
.tion between these two cases is
to compute the roll-off curve to
h densities. This is described in

:e were some way of estimating
useful for a rough estimate. Ob-
ionship between P_{50} and V_{p-p}.
ıe accurate equations described,

ɔ)
(3.32)

o the task boils down to finding
ed experimentally.

'ION

umerical modeling has been done
:cording. However, the complete
; it involves nonlinear and com-
formation details, and dynamics

: principles of the writing proce-
ıt properties and parameters. Two
of magnetization from one direc-
variability in its length, and what
ter) between such transitions. The
near density, and the second per-
iting process includes application
d in and near the gap of the head.
.e existing direction of magnetiza-
nagnetized region in the medium.
the M–H (medium magnetization
ɔ) hysteresis loop curve. The mag-
: spread-out region, and this is the
sections. Going through the step-
'ill help the practitioner know the
ics as well as appreciate the mea-

Figure 3.15 shows the building blocks of the writing process. The writing process is complex, due to time and distance factors becoming intermingled along with nonlinear magnetization process in the medium. However, it is possible to develop a sufficient qualitative understanding of the process. When digital data is written on a disk track, the medium is magnetized to saturation in one or the other direction. Incomplete or nonsaturated writing results in uneven signal outputs and causes errors. The process of writing involves a head that provides a magnetic field sufficient to reverse magnetizations in selected locations of the track. This is called *overwriting*, and its measurement is discussed in Section 8.16.

In Figure 3.15 a head and medium are shown. The medium has a magnetization in the direction of the arrow on the right-hand side of the head gap center. A current is applied instantaneously (step function) in a direction to produce a field that reverses the magnetization in the medium. Instantaneous application of current is assumed in order to clarify the basic concept. The influence of finite-time current application is considered later. The nature of the head field is described in Section 3.3, and it is shown that the x component of the head field in medium is strongest in the center line of the gap. This is also illustrated in Figure 3.15b. The field in the medium varies from x_1 to x_2. At x_1 the field is weak, while at x_2 it is strong. Corresponding to locations x_1 and x_2 in the medium, the head fields are shown as H_1 and H_2 in Figure 3.15b, and these fields are applied to the medium, resulting in magnetizations M_1 and M_2, as shown on the M–H loop in Figure 3.15c. The medium M–H loop is shown rotated 90° to simplify drawing and explanation. The magnetization M_1 at distance x_1 is too small, and only weak reverse magnetization results. At field H_2 magnetization is almost reversed close to the saturation in the reverse direction. In Figure 3.15d medium magnetization values from location x_1 to x_2 are plotted. This is the same as the transition region, and the shape of the change in magnetization is simulated by equation (3.24).

With the foregoing visualization of writing in a magnetic medium, the following points can be made:

1. The steepness of the change in the head field would influence the transition length.
2. A steep M–H loop slope can reduce transition length (a perfectly square loop is ideal).
3. The current applied to the coil to generate the H field is a function of time. If the current versus time has a shallow slope, the H field generated will be gradual. Inductance and capacitance of the head writing circuit contributes to delays in generation of fields. These factors adversely contribute to the field generation and result in elongation of transition time and length of magnetic transition. These issues become more acute at high medium velocity (RPM) and high data rates.
4. Whenever a magnetic field is changed in magnetic material, a demagnetizing field is set up in the material, and this reduces the influence of the applied field trying to magnetize the material. This is manifested in the

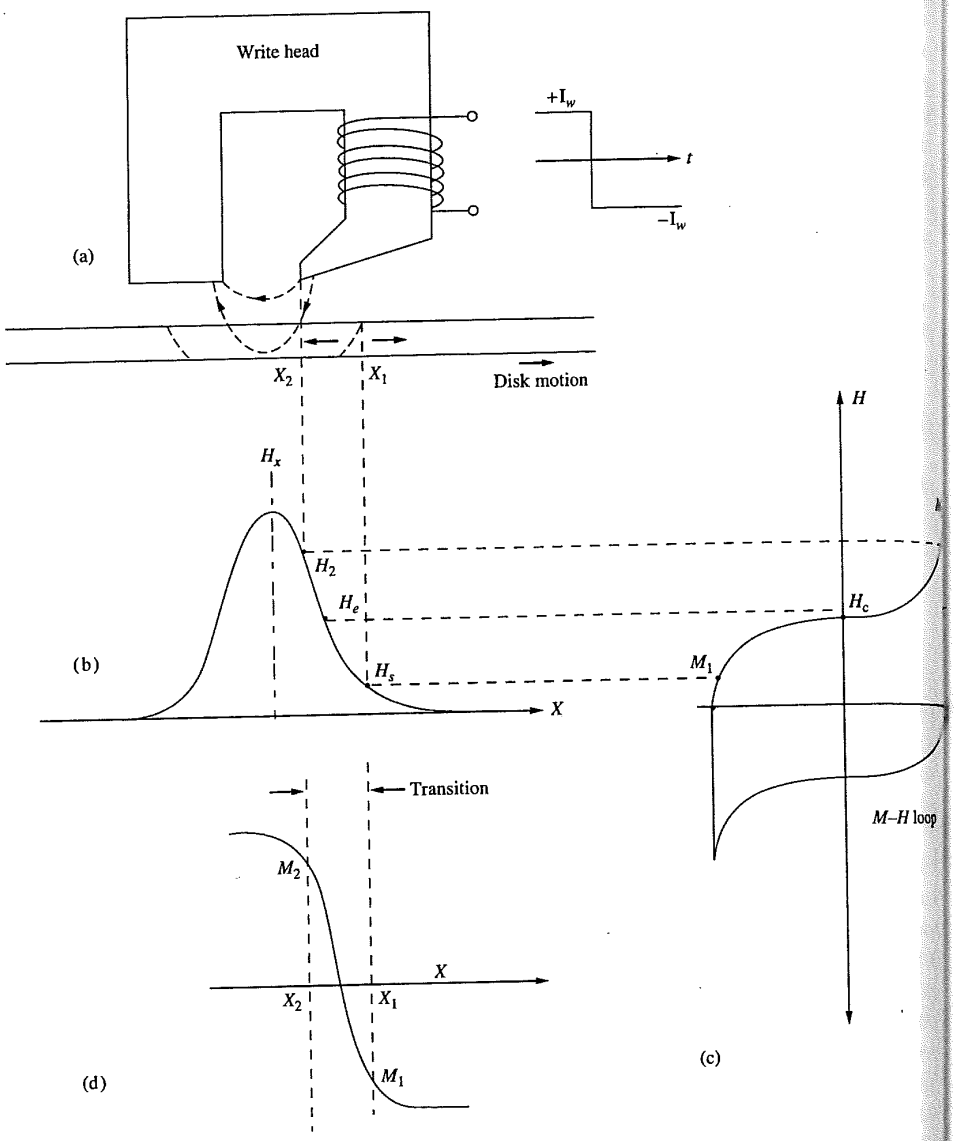

Figure 3.15 Writing process sequence.

phenomenon of "like poles repel each other." Section 2.6 describes demagnetizing fields.

Due to demagnetization fields, when the head field is supporting an already existing direction, the length of magnetization tends to elongate, and when the head field opposes the existing magnetization direction, the length of that section tends to become narrower. The discrepancies in the lengths of the segments result in variations

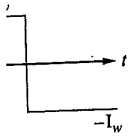

ion

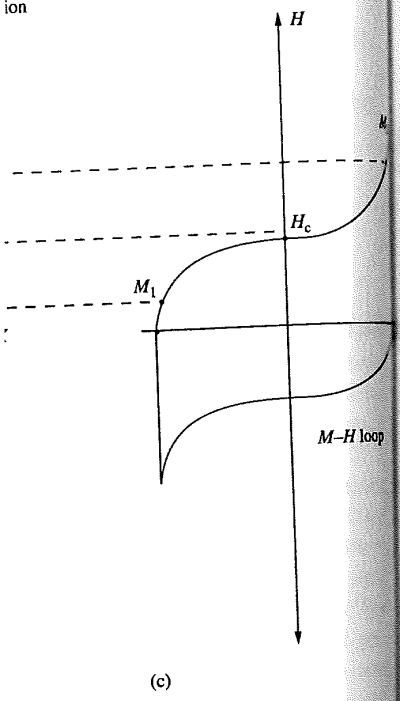

(c)

process sequence.

el each other." Section 2.6 describes

ad field is supporting an already existing
ds to elongate, and when the head field
on, the length of that section tends to be-
ngths of the segments result in variations

in locations of transition regions and create what is known as *peak jitter* in resultant sequence of signal pulses. This adversely affects linear density. As a matter of fact, the derivation of transition parameter a is based on equating a demagnetizing field slope to the applied field of the head.

3.13 SIDE WRITING, READING, ERASING, AND FRINGING FIELDS OF HEADS

In all the discussion of the magnetic field from the head and its influence on the medium so far, we have considered x and y directions. Direction x is where the head poles and gap are located, and y is the direction from the head toward the medium, as shown in Figure 3.16. For the third direction, z, we have assumed that writing and signal production occur only in the width of the head. This is a reasonable assumption for wide tracks. However, as track densities increase and tracks get narrower, the influence of fringing fields beyond the physical track width becomes important. We review this subject qualitatively with the help of Figures 3.16 and 3.17. Reference [7] gives quantitative discussion of this topic. In Figure 3.16, the axes x, y, and

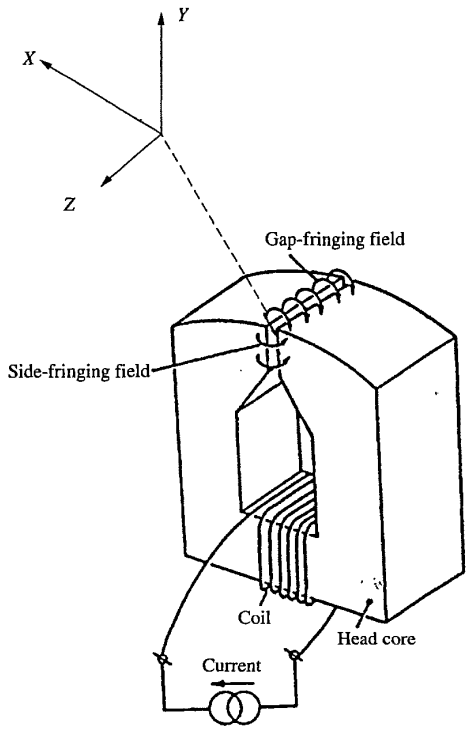

Figure 3.16 Side-fringing field of a head. [7]

Figure 3.17 Effect of fringing fields on (a) side writing, (b) side reading, (c) erase track width, (d) adjacent track crosstalk. [7]

3.14

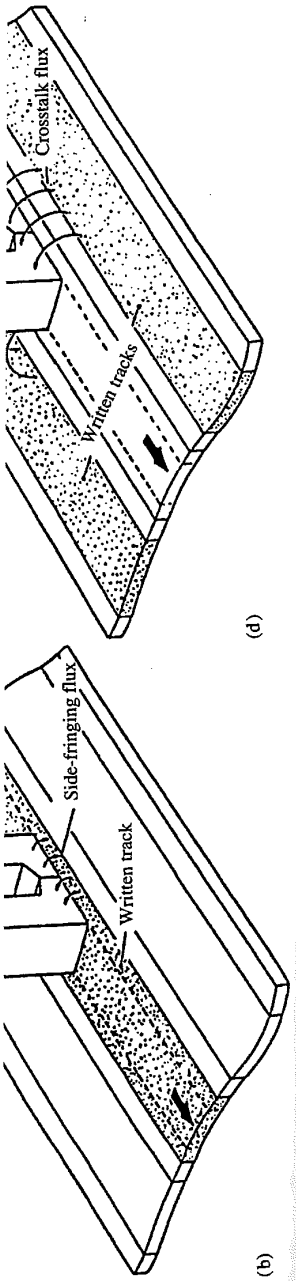

Figure 3.17 Effect of fringing fields on (a) side writing, (b) side reading, (c) erase track width, (d) adjacent track crosstalk. [7]

z are indicated. In Section 3.4, the head field in the medium at distance d is calculated. The field of at least H_c is required to reverse magnetization in the medium. However, 2.5 H_c is provided to fully saturate the medium and allow for variations in the field due to flying height, partial head saturation, and so on. For the calculation of this field, it is assumed (implicit in the Karlqvist equation) that the head is infinitely long in the $\pm z$ direction. Now if the fringe field in z at the end of the track width is viewed in a similar manner, it is seen that only half of the head surface contributes to the field, that is, the $-y$ direction. There is no head material in the $+y$ direction to add to the field. So the $H_x(0, d)$ in the z direction will be half as much as $H_x(0, d)$ in the y direction. Thus, we expect to see as much as 1.25 H_c field at distance d from the head surface in the z direction.

Currently, d, the flying height, is on the order of 100 nanometers (0.1 μm). The fringing magnetic field of $1.25H_c$ in the z direction reaches as far as 0.1 μm on both sides of the track width. Hence, the magnetic track width is effectively increased by 0.1 μm on each side of the physical track width. For writing, at least a field H_c is needed; however, the written track can be partially erased at much lower fields. So fringing fields result in erased bands on two sides of the written tracks. Influence of erase bands in the track-pitch determination are addressed in Section 9.11.

Figure 3.17 shows the influence of fringing fields during writing and reading of a magnetic track. The figure originally related to the study of fringing fields in a tape but is equally applicable to disk recording. Figure 3.17a shows how the written track width is increased from the physical head width during writing. Figure 3.17b indicates pickup of fringing fields by the read head. Figure 3.17c shows increased erase track width, which results in erase bands adjacent to written track. Figure 3.17d shows how the adjacent track signals may generate noise in the signal of a track being read. It should be noted that media parameters such as coercivity, head geometry, and the degree of asymmetry in head write and read responses influence fringing fields at track ends. Measurements of track profiles and microtrack profiles are usually carried out to relate influence of fringing fields for component integration in a drive. Chapters 8 and 9 detail some of these measurements and error rate studies.

3.14 READING SINUSOIDAL MAGNETIC TRANSITIONS

Most of the pioneering work on magnetic recording has been done on sinusoidal recording. Consumer electronics and recording utilize sine-wave signals for audio and video recording. This is changing with more and more digital techniques being used in consumer applications. For disk applications, sinusoidal signals are not used directly. However, the study of sinusoidal magnetization is useful in fundamental studies in disk recording and provides a useful insight into disk design. At

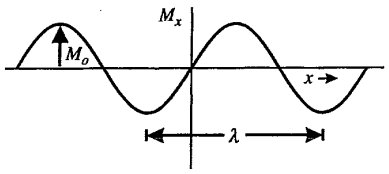

Figure 3.18 Sine-wave function.

high linear densities, digitally recorded signals become almost sinusoidal. Moreover, sinusoidal functions are convenient for analytical studies, separating the contributions of different system parameters and for referring to the literature on magnetic recording practices.

For a sinusoidally varying medium, we may write the magnetization as

$$M_x(x) = M_0 \sin(kx) \tag{3.33}$$

where x is the distance along the track and k refers to the periodicity of the magnetization and is defined by $k = 2\pi/\lambda$, where λ is the wavelength of the sine wave (Fig. 3.18). Substituting the magnetization function equation (3.33) and the Karlqvist expression for H_x from equation (3.2) into equation (3.20) and with quite a bit of algebra, Wallace [8] obtains the voltage output of the coil as

$$V(x') = -\mu_o nvw(M_r\delta)k[\eta][e^{-kd}]\left[\frac{1-e^{-k\delta}}{k\delta}\right]\left[\frac{\sin(kg/2)}{kg/2}\right]\cos(kx') \tag{3.34}$$

where $x' = vt$.

This equation explicitly separates out four loss factors as indicated by the four quantities in square brackets. The reason these terms are called "losses" is that each of these terms is smaller than unity and reduce the output voltage by a corresponding fraction. The first term is the head efficiency η and has been discussed earlier.

The second term shows that the voltage decreases very rapidly—in fact, exponentially, as the flying height d increases. This term is also known as *Wallace's spacing loss factor.* The number of decibels of power reduction due to spacing loss can be calculated using

$$\text{Spacing loss} = 20\log_{10}(e^{-kd}) = -55\left(\frac{\lambda}{d}\right)\text{dB} \tag{3.35}$$

This means that as the sinusoidal signal wavelength approaches the head-disk spacing (high frequency), the signal suffers a loss of -55 dB or the signal is reduced to less than 0.2% of its value. One practical application of the loss factor [9] is the experimental determination of flying height d in a disk drive by observing the ratio of voltages for two sinusoidal wavelengths on the disk.

The third term relates to the dependence of voltage on the medium thickness δ. The slope of this loss with increasing thickness is not as steep as that of spacing loss but is significant. This is somewhat like a spacing loss for magnetization in the medium layer. Regions of magnetization in the medium that are farthest from the

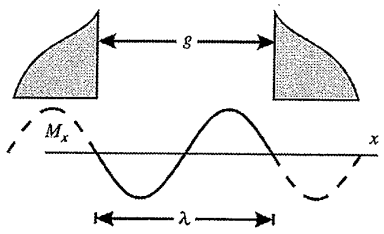

Figure 3.19 Gap loss factor.

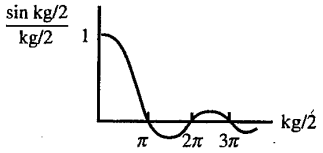

Figure 3.20 Gap nulls.

head contribute relatively little to the signal voltage. The last term in parentheses is referred as the *gap loss factor.* For a very small gap, this term is unity, and as the gap increases, the gap loss factor decreases and oscillates around zero (Fig. 3.19). The first zero corresponds to having the gap length equal to the wavelength of magnetization reversal. When this happens, there is equal positive magnetization and negative magnetization under the gap, and therefore no signal is generated (Fig. 3.20). No practical application has been considered beyond this first null. However, it has been demonstrated [10] that in the case of closely-spaced perpendicular recording transitions, a fifth null has been seen at as high as 650 kiloflux reversals per inch. This means that magnetic recording is capable of showing observable voltage signals up to very high linear densities.

REFERENCES

[1] O. Karlqvist, *Trans. R. Inst. Technol. (Stockholm),* vol. 86 (1954), p. 3.

[2] John C. Mallinson, *The Foundations of Magnetic Recording,* p. 92. New York: Academic Press, 1993.

[3] M. L. Williams and R. L. Comstock, *A.I.P. Conf. Proc.,* vol. 5 (1972), p. 738.

[4] B. K. Middleton, Chapter 2, in C. D. Mee and E. D. Daniel, eds., *Magnetic Recording Handbook.* New York: McGraw-Hill, 1990.

[5] A. S. Hoagland and J. E. Monson, *Digital Magnetic Recording,* Chapter 4. New York: John Wiley & Sons, Inc., 1991.

[6] T. Arnodussen, private communication, San Jose, (1992).

[7] A. van Herk, *"Three Dimensional Analysis of Magnetic Fields in Magnetic Recording Heads,"* Philips Research Laboratories, Eindhoen, The Netherlands, (1980), p. 40.

[8] R. L. Wallace, "The reproduction of magnetically recorded signals," *Bell Syst. Tech. J.,* vol. 30 (1951), p. 1145.

[9] B. R. Brown, H. L. Hu, K. L. Klaassen, J. J. Lum, C. L. Jacobus, J. C. L. Van Peppen, and W. E. Weresin, U.S. Patent No. 4,777,544 (1988).

[10] S. Yamamoto, Y. Nakamura, and S. Iwasaki, "Extremely high density recording with single pole perpendicular head," *IEEE Trans. Magn.,* MAG-23 (1987), p. 2070.

'idson, "Roadmap for 10 Gbit/in**2
MAG-28 (1992), p. 3078.
IBM, San Jose, CA, 1996.
films with perpendicular magnetic
l (1978), p. 849.
aterials," Addison-Wesley Publish-

8 Recording Channel

8.1 INTRODUCTION

This chapter focuses on factors that affect the linear bit density of a disk drive. On-track linear density considerations are divided into three parts:

1. The channel and its modules are described in several sections (8.2–8.14). The functions of these modules and common signal-processing steps are discussed. The concepts of peak shift or bit shift, intersymbol interference, and peak detection window are introduced. A peak detection channel is assumed for general discussion while a sampling channel is described under coding. Run length codes in current use are discussed here with primary emphasis on (1, 7) peak detection coding. Partial response, maximum likelihood (PRML) and EPRML coding are reviewed and compared with the peak detection procedure.
2. This part relates to writing and reading processes and their measurements: topics of overwrite, write current optimization, roll-off curve, and resolution are explained in Sections 8.15–8.18.
3. The topics of noise in head, electronics, and medium are discussed in this group. Signal-to-noise ratio is the important *figure of merit* used in the design and performance of the drive since it is strongly tied to the error rate of the drive. These subjects are covered in Sections 8.19–8.23.

The channel is a critical part of a disk drive system. A well-designed channel can provide superior density and performance from a drive. Innovative components

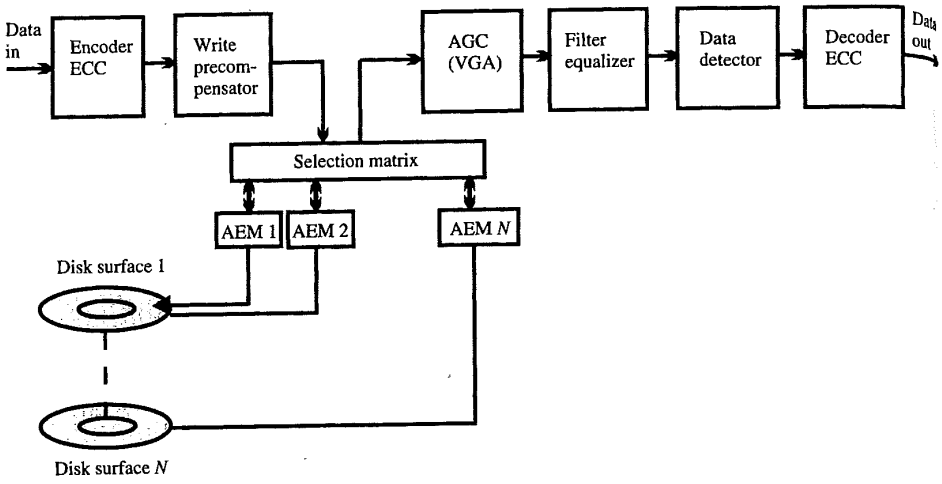

Figure 8.1 Write and read functions of a disk drive channel.

without a balanced channel can produce a substandard drive. The channel con sists of several electronic circuit modules. Figure 8.1 shows a simplified flowcha of these modules. The write encoder, precompensator, read automatic gain contr (AGC), equalizer, data detector, and decoder are common elements of the systen A multiplexor matrix located on the end of the arm (or stack) connects one head at time to these modules. These electronic modules occupied a cage of printed circu cards on the large disk drives of the 1970s. Today, all common modules are arrange on two to three semiconductor chips and efforts are under way to accommodate a the functions to one chip. The write drivers and preamplifiers are mounted in module on the arm of a head that is often referred to as the *arm electronics modul* (AEM). Every head has its own independent read/write circuits on its AEM. Th wires connecting the AEM to the heads are kept as short as possible to minimiz resistance and inductance in the circuit.

8.2 FUNCTIONS OF A CHANNEL

There are strong similarities between a communication channel and a recordi channel. Here the word "communication" encompasses several fields, such as tel phones, radio broadcasting, television, satellite transmissions, optical communic tion, and so on. The objectives are identical in all cases. The procedure to tre the data or information is almost equivalent. The information is coded to suit i transmission or storage in another medium, transferred, and later decoded to t original form. The common goal is to transfer the data from one medium to anoth and eventually retrieve it in usable form as accurately as possible with the le distortion or fewest errors.

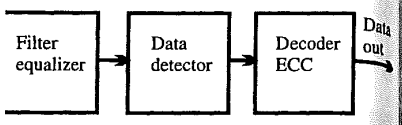

of a disk drive channel.

substandard drive. The channel con- Figure 8.1 shows a simplified flowchart mpensator, read automatic gain control er are common elements of the system. he arm (or stack) connects one head at a dules occupied a cage of printed circuit oday, all common modules are arranged orts are under way to accommodate all rs and preamplifiers are mounted in a ferred to as the *arm electronics module* nt read/write circuits on its AEM. The kept as short as possible to minimize

mmunication channel and a recording ncompasses several fields, such as tele- lite transmissions, optical communica- al in all cases. The procedure to treat it. The information is coded to suit its , transferred, and later decoded to the er the data from one medium to another s accurately as possible with the least

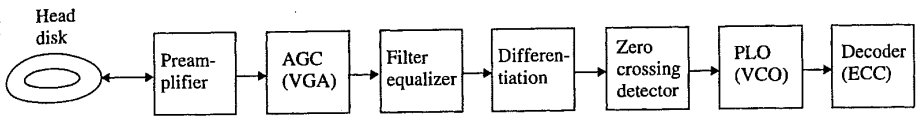

Figure 8.2 Peak detection read-process modules.

Figure 8.1 shows the writing and reading functions of a disk drive recording channel; Figure 8.2 indicates the detection process in more detail. Digital data from a computer processor or controller is first coded in a block called the *encoder*. Error correction coding is incorporated with the data at this stage. The encoded data goes through a procedure called *write precompensation*. In the next step, digital data is converted into currents by the write head drivers. This sequence of events is also depicted in a timing diagram in Figure 8.3. The head writes this sequence of pulses on disk tracks in the form of a series of transitions or magnetization changes (see Section 3.2). The rotating disk stores these transitions, and when a command to retrieve this data is received by the read head (which may be the same head that wrote the information), it transforms medium transitions into electrical voltage pulses. The information is now in analog form and includes the signal plus perturbations and noises introduced during the writing and reading processes. Detection of these signals and their conversion to digital form require several steps. Figure 8.2 and Figure 8.3 outline some of these steps.

The head output is amplified by an analog differential preamplifier. The amplification of signals is followed by automatic gain control. The automatic gain control circuit adjusts the amplitude of the signal within desirable boundaries. Next, the

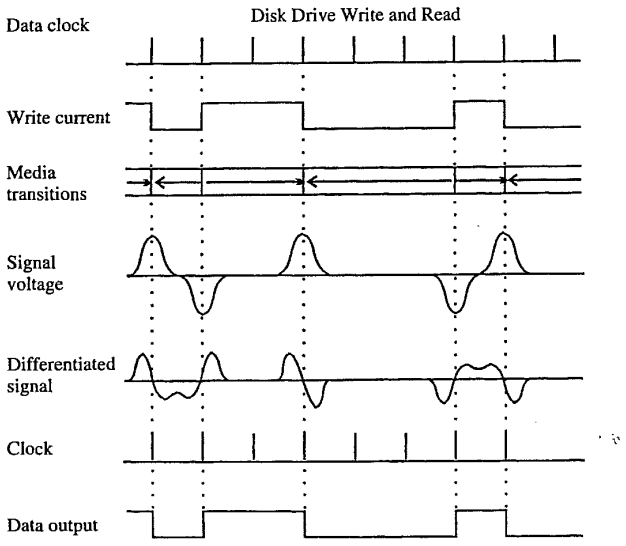

Figure 8.3 Disk drive write and read.

signal goes through low-pass filtering and/or equalization in a single module. The filtering limits the noise bandwidth, while equalization *slims* pulses so that interaction among adjacent pulses is reduced; this topic is discussed in Section 8.10. The signal is now differentiated electrically. The differentiator converts peaks of the signals into zero crossings, as shown in Figure 8.3. A comparator gate (not shown) generates pulses out of the zero-crossing-detection circuit. The leading edges of the pulses correspond to the transition locations on the medium. The series of pulses at this stage correspond to the encoded data. However, the sequence of data also contains embedded clock pulses. In the next stage, a phase-locked oscillator (PLO, also called VFO for variable frequency oscillator) monitors this embedded clock and reconstructs time intervals called *windows*. The detected zero crossings should fall within these windows. The reason for the reconstruction of clock pulses is correction of clock shifts caused by unevenness in disk rotational speed, nonlinear writing process, and noises. This topic is further discussed in Section 8.12. At the next stage, the data decoder detects the presence or absence of zero crossings within each of the windows and converts the data into its original form. This data is now in "user" bytes and the computer or controller can process it.

Figure 8.3 shows the signal processing steps described on a timing diagram. The primary function of the channel is to arrange the data for writing on the disk and retrieve it with minimum errors. The major error-causing factors in disk drive recording are as follows:

1. Intersymbol interference
2. Electronic noise from media, head, and preamplifier
3. Peak shifts generated by writing and reading processes at high bit densities
4. Overwrite loss, which relates to the effect of partially erased data
5. Effect of side writing and reading due to fringing fields at track boundaries
6. Track misregistration due to head positioning irregularities on rotating disk
7. Adjacent track interference
8. Head (magnetic) domain noises
9. Media defects.

In this chapter, the first four factors are discussed since they relate to "on-track" error-producing mechanisms. The other factors will be considered in Chapter 9 on integration. It should be noted, though, that the channel is designed to ensure error-free performance in the presence of all the factors.

8.3 PEAK SHIFT OR BIT SHIFT FROM INTERSYMBOL INTERFERENCE

When the pulse peaks deviate (shift) from the center of the expected time intervals (windows) during detection, the chances of errors increase. These peak shifts are predominantly caused by three factors:

alization in a single module. The
ation *slims* pulses so that interac-
is discussed in Section 8.10. The
erentiator converts peaks of the
. A comparator gate (not shown)
circuit. The leading edges of the
ne medium. The series of pulses
wever, the sequence of data also
, a phase-locked oscillator (PLO,
) monitors this embedded clock
ne detected zero crossings should
nstruction of clock pulses is cor-
disk rotational speed, nonlinear
liscussed in Section 8.12. At the
absence of zero crossings within
s original form. This data is now
process it.
s described on a timing diagram.
the data for writing on the disk
ror-causing factors in disk drive

reamplifier
ing processes at high bit densities
t of partially erased data
ringing fields at track boundaries
ing irregularities on rotating disk

d since they relate to "on-track"
ill be considered in Chapter 9 on
annel is designed to ensure error-

ter of the expected time intervals
s increase. These peak shifts are

1. Intersymbol interference or crowding of transitions
2. The addition of noises to the pulse waveforms by head, medium, and electronics
3. The writing processes.

In this section, the first cause, intersymbol interference (ISI) is discussed. Figure 8.4a shows read pulses from two isolated transitions. As these transitions are brought closer (at higher linear bit densities), the pulses due to the two transitions superimpose, as in Figure 8.4b. Note that (1) the resultant double-pulse peaks are reduced in amplitudes and (2) the location of signal peaks has been shifted outward as if the peaks have been "repelled" by each other. The reductions in amplitude of pulses cause a roll-off curve, discussed in Section 8.18. The shift in peaks is important since excessive shift tends to make the peak fall outside of its designated time interval during peak detection. In the figure, it is assumed that two pulses can be superposed linearly. As crowding becomes severe, the peak shift increases. When the peak shifts exceed 10–20% of clock window, error rates become excessive. There are several techniques that reduce the crowding and bit shifts. Equalizing or slimming the pulses is one method (Section 8.10), and an appropriate coding scheme (Section 8.5) is another. The amounts of shifts can vary depending on the sequences of 1's and 0's. However, there is some predictability of shifts in coded data, and it is used to reduce shifts by precompensated writing, as explained in Section 8.7.

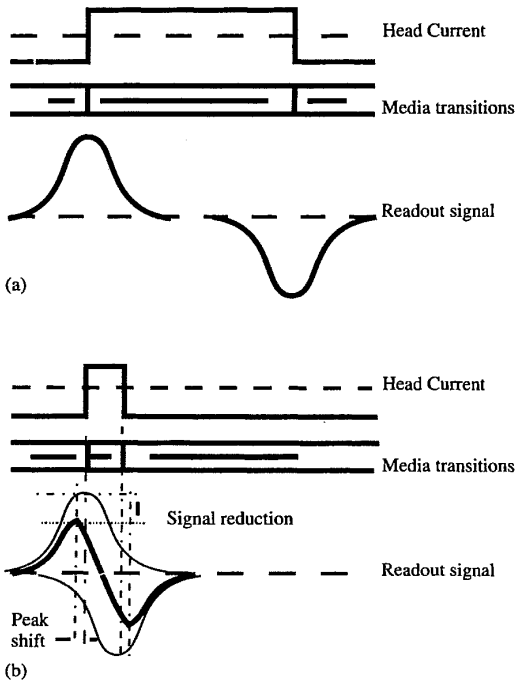

Figure 8.4 Intersymbol interference (a) low density, no ISI (b) high density, ISI and peak shift.

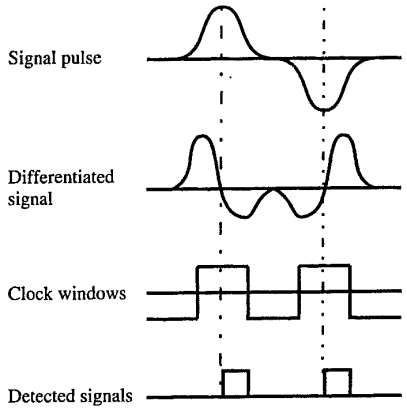

Figure 8.5 Peak detection window.

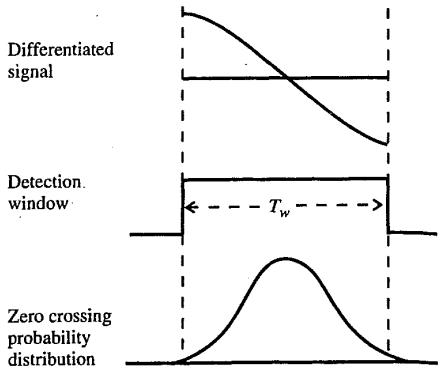

Figure 8.6 Peak detection window and peak jitter distribution.

8.4 PEAK DETECTION WINDOW

Figure 8.5 shows the signal pulses, differentiated signals, designated windows, and detected signals. The listed factors in Section 8.2 contribute to deviations in the location of a bit zero crossing in a window. Since there are several factors influencing the location of a signal peak or zero crossing, it is convenient to think of the position of peak as a statistical outcome. The position of the peak, on average, may fall at the center of the window. It may fall within or outside the window with various probabilities. The probability of the peak falling outside of a window interval denotes errors. Section 9.13 describes the translation of error probability into error rates. The following discussion addresses how the error probabilities may be calculated.

Location of the peak window has a distribution of the type shown in Figure 8.6. The mean or average location of the peak may be in the center. The distribution may be assumed to be normal or Gaussian with a mean at 0, the center of the window, and a standard deviation of σ. Normal distribution fit is an idealization that allows for analytical calculations. More critical application may need experimentally derived distribution. The probability that the bit peak falls outside of the window is given by the area of the curve outside of window boundaries. For low error rate or low probability of error, the distribution should be narrow with small σ. In this chapter, only factors causing peak jitters due to on-track variables are considered. Chapter 9 describes additional factors that cause peak jitter due to off-track variables.

8.5 CODING IN A DISK DRIVE CHANNEL

The procedure of coding for a disk drive is simply a conversion of incoming "user bits" into another bunch of bits with an objective of promoting high linear density while reducing errors. Figure 8.7 depicts the encoding process.

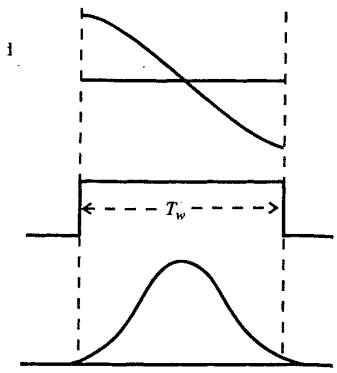

Peak detection window and peak jitter distribution.

d signals, designated windows, and
2 contribute to deviations in the lo-
here are several factors influencing
convenient to think of the position
he peak, on average, may fall at the
ide the window with various prob-
side of a window interval denotes
f error probability into error rates.
or probabilities may be calculated.
ion of the type shown in Figure 8.6.
in the center. The distribution may
1 at 0, the center of the window, and
it is an idealization that allows for
may need experimentally derived
lls outside of the window is given
ndaries. For low error rate or low
urrow with small σ. In this chapter,
variables are considered. Chapter 9
r due to off-track variables.

ly a conversion of incoming "user
e of promoting high linear density
coding process.

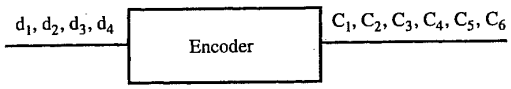

Figure 8.7 Customer data and coded bits.

The bits on the output side of the encoder are used by the write driving circuit to initiate and control head coil currents. Early disk drives relied on the very simple procedure of writing user data directly onto the disk. This procedure is a form of coding in which the C's are the same as the d's, or $C_i = d_i$. Figure 8.8a shows this code, known as nonreturn to zero (NRZ). The reason for the name is that the current is always in either a positive or a negative direction during writing but never at zero (the dashed baseline). The figure shows data pattern 011010 and clocking intervals. The NRZ-coded bit pattern corresponds to the direction of currents in the write head. The resultant magnetization transitions in the disk medium are also shown.

Every coding scheme has "rules" that allow construction of coded bit patterns. In the case of the code in Figure 8.8a, whenever the data bit changes from 0 to 1, the write coil current goes from negative to positive, and the magnetization reverses direction from left to right. For one or more 1's, the current continues in the same direction; hence, magnetization in the medium continues in the left-to-right direction. When incoming data bits change from 1 to 0, the current in the write coil reverses, creating the transition in the medium. For the duration of 0's, the current and magnetization

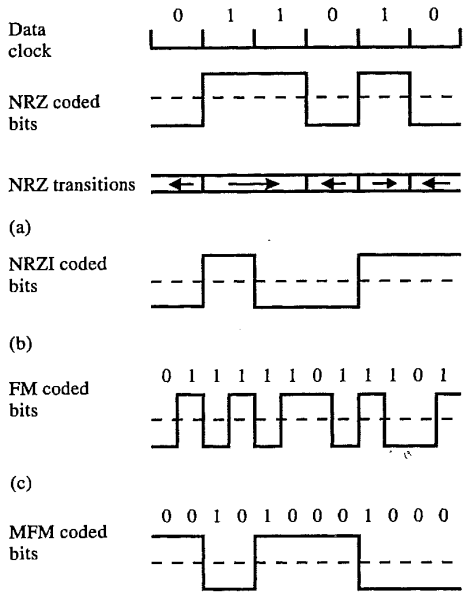

Figure 8.8 Codes and magnetic transitions.

continue to remain in the same direction. Although this is the simplest form of coding, it has several disadvantages. First, the number of transitions on the disk track are the same as the number of incoming user bits; other schemes can store more bits with fewer transitions. Second, when a long series of 0's exists in the user data, there is no clocking information in the data. Hence, the data flow cannot be used for re-creating clock pulses. Third, if there is an error in any bit of the NRZ method, the error propagates by reversing transitions erroneously.

8.6 NRZI, MFM, AND RUN LENGTH–LIMITED CODES

The procedure of coding called nonreturn to zero inverted (NRZI) is a modification of NRZ discussed earlier. It removes one of the disadvantages of the NRZ scheme. Figure 8.8b shows this method. The rule here is that, at every clock position, if the data bit is 1, the direction of the current changes, and hence the medium magnetization reverses, creating a transition at that time. Thus, transitions in the medium are synchronized with the occurrence of 1's in the data sequence. In this case, an error in any one bit can be spotted, and hence it can be corrected. The code cannot provide reliable clocking when there are many 0's in a sequence and the density of transitions is the same as the incoming data bits. These simple codes may be used as standards for comparisons with other codes used for disk drive applications.

The two methods just discussed actually involve no encoding. One major reason for encoding data prior to writing on the disk is to pack more user data on a disk. Once the maximum transition density on a disk track is determined, coding allows more user bits without exceeding allowed transition density. Another objective of coding is to rearrange the incoming data so as to reduce the possibility of errors during writing, reading, and detection. The third function of the coding procedure is to ensure that when data is read from the disk track, the sequence of coded bits should allow re-creation of timings or generation of the clock so that data detection is more accurate and self-clocking. Two codes meet this requirement. The first one is known as a frequency modulation (FM) code and is not used much for disk drives, but it is a useful stepping-stone to the understanding of the very popular MFM code.

8.6.1 FM

The objective of this code is to make itself self-clocking simply by inserting 1's between every two user bits. Figure 8.8c shows the string of user data bits converted according to this rule. The bit-reversal diagram indicates clocking bits added to the code bits. The presence of 1's at expected locations simplifies clocking. The read and write clocks have to run at twice the frequency of data bits to accommodate these additional inserted 1's. The other disadvantage of the code is that the maximum number of transitions per unit distance are twice as large as those in NRZ/NRZI coding. The window within which detection must take place is half as wide as NRZ or NRZI codes.

8.6.2 MFM

The modified frequency modulation code is also known as the Miller code. Figure 8.8c reveals that there are many more transitions than necessary to break up a string of 0's for making the code self-clocking. In other words, the FM code is "extravagant" for the objective of self-clocking. A new code was invented (Figure 8.8d) that met the following two conditions:

1. At least one 0 must exist between any two 1's so that transitions are minimized.
2. No more than three 0's must exist between any two 1's.

This latter constraint avoids a long stream of 0's, making self-clocking possible. Such a code is MFM [or (1, 3)]. The process of finding the "rules" to encode data from user bits to accomplish the foregoing objectives gets a little complex. However, the procedures for encoding data according to this and other run length–limited (RLL) codes has been well established and described in the literature [1, 2]. We shall not go into these methods. Still, it is important to understand some of the attributes of the most commonly used codes. Looking at Figure 8.8d, one can confirm that the constraints described earlier are really met in the MFM coded bits. The minimum distance between any two coded bits is two clock cycles due to the rule that there should be at least one 0 between two 1's. As a result of this condition, the intersymbol interference or crowding of the pulses is two times less than FM code and equal to NRZI code. However, the MFM code requires the same clocking frequency as the FM code or twice the frequency of user data bits or NRZI. The window within which the coded bit should be detected is half as small as in the case of NRZI. Hence the code is a hybrid of NRZI and FM codes with some advantages of both. For the analysis of attributes and comparisons among codes, a system of nomenclature has been developed. Let us define these terms with MFM code as an example. Figure 8.9 is redrawn from Ref. [2] for the comparison of codes with a 4-bit data sequence. This figure is helpful in clarifying attributes for most used codes.

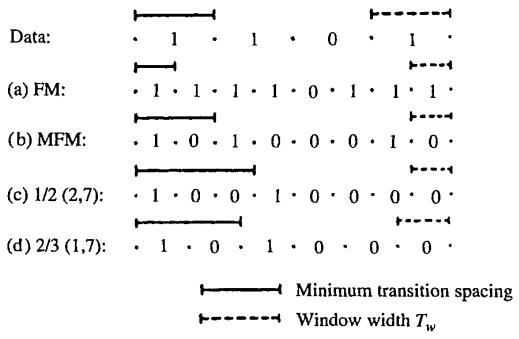

Figure 8.9 Run length–limited code patterns [2].

When x bits are encoded into y code bits, the ratio x/y is called the *code rate*. Note that y should always be larger than x if the coded data is to be constrained. This can be explained by the fact that x bits result in 2^x possible sequences and coded y bits result in 2^y sequences. The number of coded sequences should be larger than the user bit sequences so that the remaining sequences can be utilized to conform to constraints imposed by the code. In the case of MFM, the code rate is 1/2, since 4 user data bits are converted into 8 coded bits, as observed in Figure 8.9b. The minimum number of 0's required (in coded bits) between any two 1's is assigned the letter d, while the maximum number of 0's allowed between two 1's is given the letter k. For MFM, $d = 1$ and $k = 3$. The code is defined by these quantities as $x/y\,(d, k)$. So the MFM code is characterized by 1/2 (1, 3). Note that NRZI can be recognized as 1/1 (0, ∞) code. The quantity d of the code relates to the minimum distance between transitions. The higher the value of d, the longer the time intervals between transitions. The parameter k relates to the allowed length of time intervals in 0's before the clocking procedure becomes ineffective.

If the clock interval T is one cycle of the data bits, the coded clock time interval is given by $(x/y)T$. This is also the time interval within which the coded bit must be detected; hence,

$$T_w = \left(\frac{x}{y}\right)T \tag{8.1}$$

For MFM code, $T_w = (1/2)T$. The minimum time intervals between transitions $T_{\min}$ for coded data can be given by referencing Figure 8.9 as

$$T_{\min} = (d + 1)T_w = (d + 1)\left(\frac{x}{y}\right)T \tag{8.2}$$

The MFM code minimum transition time $T_{\min} = 2(1/2)T = T$. One of the most useful quantities relating user bit density in bits per millimeter (b/mm) to the flux changes per millimeter (fc/mm) on the disk track is defined as a density ratio and is given by the ratio of reciprocals of time intervals as

$$\frac{\text{b/mm}}{\text{fc/mm}} = \frac{1/T}{1/T_{\min}} = (d + 1)\frac{x}{y} \tag{8.3}$$

The density ratio for the MFM code is 1; hence, fc/mm on the disk is equal to b/mm. One more quantity of interest is the ratio of the highest possible frequency content to the lowest frequency content of any specific code and is given by

$$\frac{f_h}{f_l} = \frac{k + 1}{d + 1} \tag{8.4}$$

This quantity is useful for carrying out write-over loss and resolution measurements, described later in the chapter. A method of deriving maximum frequency of

the ratio x/y is called the *code rate*,
coded data is to be constrained. This
2^x possible sequences and coded y
led sequences should be larger than
quences can be utilized to conform
of MFM, the code rate is 1/2, since
s, as observed in Figure 8.9b. The
s) between any two 1's is assigned
s allowed between two 1's is given
code is defined by these quantities
d by 1/2 (1, 3). Note that NRZI can
l of the code relates to the minimum
ue of *d*, the longer the time intervals
the allowed length of time intervals
neffective.
ta bits, the coded clock time interval
al within which the coded bit must

(8.1)

time intervals between transitions
Figure 8.9 as

$$l + 1)\left(\frac{x}{y}\right)T \qquad (8.2)$$

$= 2(1/2)T = T$. One of the most
s per millimeter (b/mm) to the flux
ck is defined as a density ratio and
vals as

$$(d + 1)\frac{x}{y} \qquad (8.3)$$

fc/mm on the disk is equal to b/mm.
highest possible frequency content
code and is given by

(8.4)

over loss and resolution measure-
of deriving maximum frequency of

a head-disk system is exemplified. Assume a disk velocity of 10 m/s and a medium density of 2000 fc/mm with a pattern of all 1's. The number of transitions traversing per second under the head is $10 \times 10^3 \times 2000$. Two transitions make one cycle. Hence the high frequency of data is 10 MHz.

8.6.3 RLL Codes

IBM introduced the run length–limited code 1/2 (2, 7) in its 3380 disk drives in 1980. This became an industry standard in all major large-size drives. As illustrated in Figure 8.9c, the clock frequency of the coded data is twice the data bit density, similar to the MFM code. The time interval window T_w is one-half of the data clock time interval. The minimum two 0's between the 1's result in $T_{\min}$ of 3/2 T. The density ratio for the code is (b/mm)/(fc/mm) = 3/2. Thus 50% more user bits are stored in a given number of flux transitions compared to MFM. The constraint of seven maximum 0's between 1's allows a sufficient rate of transitions to extract clock information from data.

Lately, a 2/3 (1, 7) code has become the standard for all sizes of disk drives. This code maps 4 bits of user data into 6 bits of coded data so the code rate is 2/3. The clock window to detect coded data is $T_w = 2/3T$, about 33% larger than that in 1/2 (2, 7) code. The code clock rate is 50% faster than the data bit clock frequency, making electronics less limiting than the 1/2 (2, 7) code where the required clock rate was twice the frequency of the data clock. The minimum time interval between transitions is $T_{\min} = 4/3T$ and the density ratio bpi/fci = 4/3, about 11.3% less advantageous than the (2, 7) code. Figure 8.9d shows the attributes of the code in comparison with other codes.

We conclude this section on coding by presenting Table 8.1, which summarizes attributes of the codes discussed and includes corresponding information for PRML code as well.

TABLE 8.1 Disk Drive Recording Codes and Their Parameters

Code	Code Rate, x/y	Detection Window, T_w	Transition Time, $T_{\min}$	(b/mm)/ (fc/mm)	bpi/ (fc/mm)	Clock Frequency Ratio	f_h/f_i
NRZI 1/1 (0, ∞)	1/1	T	T	1	25.4	1	—
MFM 1/2 (1, 3)	1/2	1/2 T	T	1	25.4	2	2
1/2 (2, 7)	1/2	1/2 T	3/2 T	3/2	38.1	2	8/3
2/3 (1, 7)	2/3	2/3 T	4/3 T	4/3	33.87	1.5	4/1
PRML 8/9 (0, 4, 4)	8/9	0.89 T	0.89 T	0.89	22.6	1.11	4/1

8.7 WRITE PRECOMPENSATION

Section 8.3 described ISI and peak shifts due to transition crowding. The last section discussed coding schemes that reduce transition crowding by inserting the number of 0's between 1's and widening the window of detection. The equalization discussed in Section 8.10 uses electronic signal processing to slim down the pulses and thus reduce ISI. This section describes another method, called *write precompensation*, to reduce intersymbol interference. Write precompensation, often referred to as *write equalization*, is a significant step practiced to reduce peak shifts in coded data. During the write process, the current pulses that write the data can be timed to compensate for peak shifts occurring during reading. The shifting of peaks depends on the coded bit patterns and density of transitions. It is desirable to have the pulse peaks fall in the center of the detection windows for minimum errors. Peak shifts with worst case data patterns at the inner diameter of the disk (where the density of transitions is highest) can cause the worst error rates.

Referring to Figure 8.4b, the current in the write coil for transition that corresponds to the positive pulse is delayed by the estimated shift interval, while the write current for the trailing, negative pulse is shifted ahead by the expected shift amount. This procedure is called *write precompensation* and is successfully applied in many drives. One would think that for different sequences of bits there would be a variety of bit shifts (the words *bit shift* and *peak shift* are used interchangeably), and it would be difficult to apply a standard compensation for possible cases. Actually, there are only a few combinations of data that require different degrees of precompensation. The estimated precompensation algorithms may be stored in look-up tables. The process of precompensation brings data pulses closer, and hence it increases the frequency content of the signal, which is also the characteristic of read equalization. For this reason, the procedure is also called *write equalization*. There is some penalty of increased noise in the channel due to widening of the frequency bandwidth.

8.8 ARM ELECTRONICS MODULE

Figure 8.1 shows the schematics of a multihead disk drive system. The arm electronics module encompasses the following functions in the read and write operations of the drive:

1. There are circuits that switch a head between the write and read operations.
2. The write drivers supply fast switching currents to the head according to the data input.
3. The preamplifier circuits amplify small readout signals.
4. The MR head requires constant-current- or constant-voltage-supply circuits to activate the sensor.

The arm electronic circuit schematic for an inductive head is shown in Figure 8.10

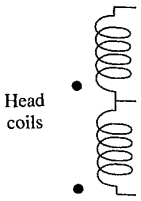

Figu

The AEM is l
addition of ind
write driver fo
procedure to se

For writi
write drivers. I
wide-bandwid
adding signific
gets amplified
of 100. Once t
significant noi

Resistor
reduces oscill
versus-output-
application. E
are treated in

8.9 AUTOMATIC G

The function
signal values
detection proc
before the det
stage is measu
as to maintain
of the reasons

1. Flyin
2. Disk
3. Medi

nsition crowding. The last section
rowding by inserting the number
detection. The equalization dis-
ssing to slim down the pulses and
ethod, called *write precompensa-*
ecompensation, often referred to
ed to reduce peak shifts in coded
hat write the data can be timed to
ng. The shifting of peaks depends
s. It is desirable to have the pulse
for minimum errors. Peak shifts
of the disk (where the density of
tes.
write coil for transition that cor-
stimated shift interval, while the
ifted ahead by the expected shift
sation and is successfully applied
nt sequences of bits there would
peak shift are used interchange-
compensation for possible cases.
ata that require different degrees
ion algorithms may be stored in
ings data pulses closer, and hence
which is also the characteristic of
is also called *write equalization.*
channel due to widening of the

lisk drive system. The arm elec-
ons in the read and write opera-

en the write and read operations.
urrents to the head according to

eadout signals.
or constant-voltage-supply cir-

ve head is shown in Figure 8.10.

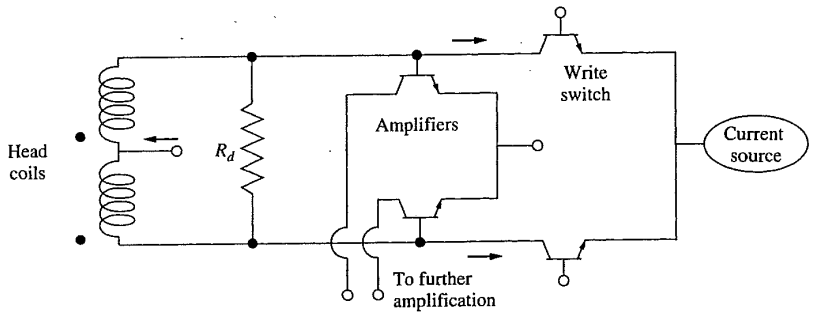

Figure 8.10 Arm electronics schematic—current driver and preamplifier.

The AEM is located on the head arm as close to the head as possible to reduce addition of inductance, resistance, and capacitance to write/read circuits. A typical write driver for a center-tapped ferrite or film head is shown in Figure 8.10. The procedure to select the optimum write current is described in Section 8.17.

For writing, signal input from the precomp circuit is applied to the base of the write drivers. For reading, the signal output is differentially applied to the bases of wide-bandwidth, low-noise transistors. This stage should amplify the signal without adding significant noise to it. Note that any noise added to the signal at this stage gets amplified along with the signal. The gain of a typical amplifier is on the order of 100. Once the signal is large enough, the later stages of amplification do not add significant noise to the detection process.

Resistor R_d has a dual function. During writing, it provides damping and reduces oscillations in the output current. During reading, it flattens the frequency-versus-output-voltage profile and reduces the effect of resonance for wide-bandwidth application. Equivalent circuits and performance of the ferrite, film, and MR heads are treated in Section 5.7.

8.9 AUTOMATIC GAIN CONTROL MODULE

The function of the AGC is to adjust the gain of read peak voltages so that the peak signal values going into detection circuits are within tolerable levels for the peak detection process. This is accomplished by means of a monitoring feedback loop before the detection stage to the AGC module. The voltage prior to the detection stage is measured and fed back to the variable gain amplifier. The gain is adjusted so as to maintain a detection voltage within a specified range. The following are some of the reasons for the variability in the magnitude of incoming voltage signals:

1. Flying height changes
2. Disk-to-disk and head-to-head variations
3. Medium coating thickness, and media remanence variations.

The AGC feedback loop is designed so that it corrects only slowly varying (low-frequency) changes but is not responsive to the high-frequency content of the signal gains. The sudden changes in signal would be undesirable since they can create distortion in signals and peak shifts.

8.10 FILTER AND EQUALIZER

The function of a low-pass filter following the AGC module is to limit high frequencies, thereby limiting noise entering the detection process. The noise is proportional to the total bandwidth of the signal, and reduction of bandwidth by high-frequency cutoff reduces noise added to the signal. The filter bandwidth should be sufficient to allow signal content. The filter cutoff frequency can be estimated from the rule that it should be equal to two times the highest frequency of recorded transitions. For example, the IBM 3380 disk drive data rate was 3 MB/s or 24 Mb/s (assuming 8 bits/byte). The drive used (2, 7) code; hence, 24 Mb/s translates into 16 Mfc/s (look at the (b/mm)/(fc/mm) ratio in Table 8.1). Two flux changes make a cycle; hence, the highest frequency of flux changes is 8 MHz, and a filter cutoff frequency of 16 MHz (at -3 dB) may be used. For (1, 7) coded data, the filter cutoff frequency (in MHz) is given by the data rate in MB/s times 6. For example, a 4.5-MB/s data rate with (1, 7) coded channel would produce a filter cutoff of 27 MHz. The fifth-order Butterworth filter is often used to provide reasonably sharp cutoff with linear phase response [3]. The filter provides a more symmetrical pulse, thereby reducing noise and, depending on the specific design, providing partial equalization.

Equalization is an electrical technique of slimming signal pulses so that intersymbol interference among adjacent pulses is significantly reduced. Chapter 5 discussed thin pole, thin film heads. Thin poles in these heads result in undershoots to the signal pulse. The undershoots tend to slim the pulses and provide built-in equalization. An interesting aspect of this type of built-in equalization is that it is "adaptive"; that is, the slimness varies according to the linear velocity as the head moves from the inner diameter to the outer diameter. Ferrite heads, MR heads, and thick pole film heads do not have significant built-in slimming or equalization. In most circumstances, these heads can benefit from electronic equalization. First, the process of shaping the pulses with equalization process is described; then the advantages and shortcomings of using equalization are discussed. Considerable work has been done and reported on the art of designing equalization for communication and magnetic recording channels. Here the principle of equalization for disk drives is explained in a simplified form. Figure 8.11a shows a pulse of voltage read from the disk transition. Figure 8.11b shows short pulses replicated from the pulse in Figure 8.11a and placed at different time locations. The summation of pulses in Figures 8.11a and 8.11b is shown in Figure 8.11c. The resultant pulse is slimmer. This and a more complex form of equalization synthesis are conveniently carried out by using a delay line with taps.

corrects only slowly varying (low-
igh-frequency content of the signal
undesirable since they can create

GC module is to limit high frequen-
ı process. The noise is proportional
n of bandwidth by high-frequency
r bandwidth should be sufficient to
can be estimated from the rule that
uency of recorded transitions. For
s 3 MB/s or 24 Mb/s (assuming 8
Mb/s translates into 16 Mfc/s (look
flux changes make a cycle; hence,
and a filter cutoff frequency of 16
lata, the filter cutoff frequency (in
For example, a 4.5-MB/s data rate
cutoff of 27 MHz. The fifth-order
ably sharp cutoff with linear phase
ical pulse, thereby reducing noise
partial equalization.
slimming signal pulses so that in-
s significantly reduced. Chapter 5
ı these heads result in undershoots
n the pulses and provide built-in
f built-in equalization is that it is
; to the linear velocity as the head
ter. Ferrite heads, MR heads, and
lt-in slimming or equalization. In
ı electronic equalization. First, the
process is described; then the ad-
are discussed. Considerable work
ing equalization for communica-
principle of equalization for disk
.11a shows a pulse of voltage read
t pulses replicated from the pulse
ions. The summation of pulses in
c. The resultant pulse is slimmer.
ynthesis are conveniently carried

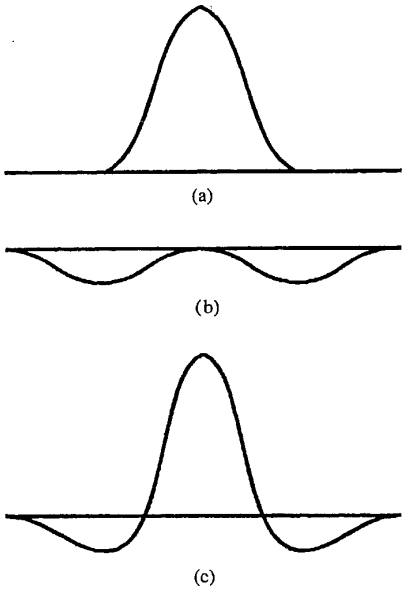

Figure 8.11 Equalization process: (a) unequalized signal, (b) fractional signals, (c) equalized (slimmer) signals.

Figure 8.12 shows a tapped delay line. The output equalized voltage pulse is given in terms of input pulse, delay times, and reduction factors of the pulse. The process indicated in Figure 8.11 is now explained in terms of input and output of the delay line, Figure 8.12. The input signal is as shown in Figure 8.11a. In the delay line A_1 represents reduction and reversal of the original signal by a factor $-a$; this represents the left-hand, short reversed signal in Figure 8.11b. For the example here A_2 is 1, that is, the unchanged magnitude of the input signal occurring at a time D after the input. Here, A_3 is again $-a$, so that the replica of the original reduced and reversed signal appears at the output after a time delay of $2D$ and represents the right-hand side of the signal in Figure 8.11b. The summation of signals occurring in these magnitudes and delays results in the output shown in Figure 8.11c. Other delay line taps are unused. This process is next indicated in analytical form:

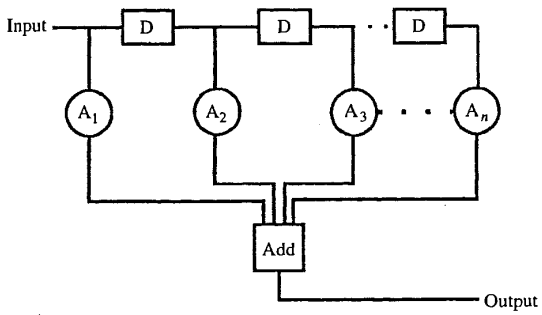

Figure 8.12 Equalization with a tapped delay line.

$$v_0(t) = -av_i(t) + v_i(t - D) - av_i(t - 2D) \tag{8.5}$$

The Fourier transform of this equation converts it into frequency domain as

$$V_0(j\omega) = (-a + e^{-j\omega D} - ae^{-j\omega 2D})V_i(j\omega) \tag{8.6}$$

For a specific case of $a = 0.5$, the equation can be rewritten as

$$\frac{V_0(j\omega)}{V_i(j\omega)} = [1 - \cos(\omega D)]e^{-j\omega D} \tag{8.7}$$

The ratio of the output voltage to the input voltage in the frequency domain is called a *transfer function of equalization.* This transfer function is referred to as a *cosine equalizer* [4]. The equalized pulse waveform for $a = 0.22$ and several values of delays D in nanoseconds are shown in Figure 8.13 [3]. The selection of specific values of a's and D's involves trade-offs between improvements in ISI and increased noise due to the increased bandwidth. The signal bandwidth and noise voltage are discussed in Section 8.19.

As indicated earlier, much work has been done on the synthesis of equalizers for optimum designs for rigid-disk drive applications. Semiconductor chips are available that allow programming of coefficients of tapped delay lines for optimizing applications. However, it should be noted that equalized signals require increased frequency bandwidth and result in the addition of noise to the signal. The transitions and pulses are most crowded at the innermost diameter. As a head reads increasing-diameter tracks, pulse crowding is reduced. For optimum results, equalization needs to be varied accordingly.

Due to the complexity of electronics and addition of noise, equalization was rarely used in large drives. Write precompensation combined with low-pass filtering has been sufficient for most applications. With thick pole, thin film heads and MR heads, equalization is routinely used. Use of PRML channel requires shaping of a signal pulse with carefully designed filtering.

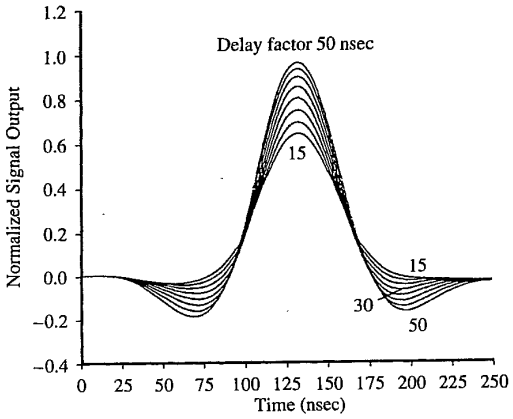

Figure 8.13 Film head equalization: $a = 0.22$; $D = 15 \cdots 50$ ns [3].

8.11 PEAK

$w_i(t - 2D)$ (8.5)

to frequency domain as

$^{\omega 2D})V_i(j\omega)$ (8.6)

ewritten as

$^{-j\omega D}$ (8.7)

the frequency domain is called
ıction is referred to as a *cosine*
= 0.22 and several values of
]. The selection of specific val-
ovements in ISI and increased
ındwidth and noise voltage are

ıne on the synthesis of equal-
ications. Semiconductor chips
s of tapped delay lines for op-
that equalized signals require
ddition of noise to the signal.
innermost diameter. As a head
reduced. For optimum results,

tion of noise, equalization was
ımbined with low-pass filtering
pole, thin film heads and MR
channel requires shaping of a

c

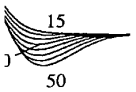

75 200 225 250

; $D = 15 \cdots 50$ ns [3].

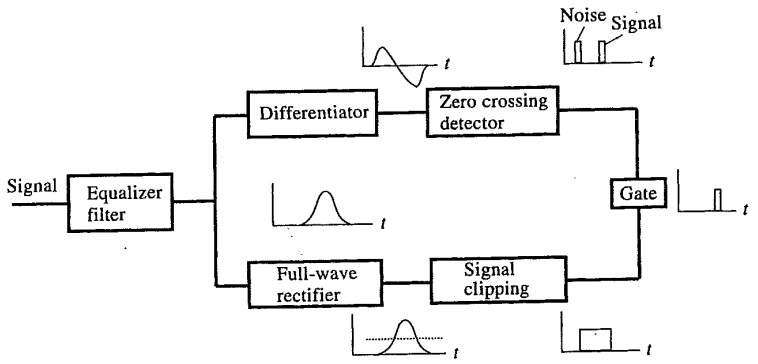

Figure 8.14 Zero crossing peak detection with clipping.

8.11 PEAK DETECTION PROCESS

In Section 8.4, on the peak detection window, the general procedure of obtaining a differentiated zero crossing signal in the window for detection was described. This section will discuss in some detail the process with a gated peak detection technique (Figure 8.14). The objective of the procedure is to detect signals accurately by eliminating the effect of low-level baseline noise and spurious noises introduced by medium surface irregularities. The coded signal passes through two parallel paths. In one path the signal goes through differentiation. Differentiation of the pulse results in the waveform with a zero crossing at the peak location. Detection of zero crossing within time window signifies a signal or "1." However, the detection process must also satisfy a second condition, discussed below.

Figure 8.14 shows the output passing through an *and* gate. The second path followed by the original signal is shown in the lower part of the figure. The isolated pulses in this path are rectified by a full-wave rectifier. As a result, all positive or negative peak waveforms are now converted into positive pulses. The rectified pulses go through a process called *clipping*, which only allows peaks larger than the designated clipping voltage. The purpose of clipping is to ensure that low-level noises are eliminated from the pulse sequence and only sufficiently large signal pulses go through. The signals from two parallel paths are logically *anded*, which means only signals that occur simultaneously in both paths are accepted as legitimate signals. Spurious noise (shown in the upper path) is not accepted as valid since the same noise signal is not present in both branches of the parallel paths after baseline noise is clipped. The procedure thus assures that only pulses larger than the designated magnitude generate output.

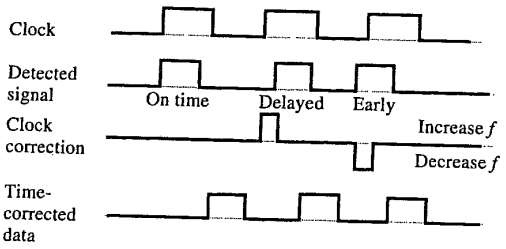

Figure 8.15 Clock correction at PLO module.

8.12 VARIABLE FREQUENCY OSCILLATOR OR PHASE-LOCKED OSCILLATOR

The function of this stage is to ensure that the read-back clock is in synchronization with the read data. Section 8.5 pointed out that the codes have embedded the clock within the data. The constraint on the code ensures that periodic pulses will appear. Digital clock pulses generated from the data are compared with the standard clock determining window timings. Any discrepancies between the two are corrected by the PLO so that data pulses are detected within corresponding detection windows.

Figure 8.15 shows a simplified process of the data timing correction. Differences between the detection window clock and data timings are registered, and a difference signal is averaged over several bits. The phase-locked loop now modifies the clock frequency according to the average effect of the required correction. The same feedback loop also modifies individual data pulse timings according to short time corrections as required. The modification of clock frequency responds only to relatively long time durations, while corrections to data intervals take place on a pulse-by-pulse basis.

8.13 PARTIAL RESPONSE MAXIMUM LIKELIHOOD CHANNEL

The acronym PRML is derived from the data communication field. The term PRML stands for two separate concepts: PR for partial response and ML for maximum likelihood. It is possible to use a non-PR code such as (1, 7) with sampling and maximum likelihood detection. The next section discusses the principle of this concept. First, we shall discuss the attributes of and motivations of using a PRML channel. Next, a simple explanation of the concept is given along with a comparison between peak detection and PRML channels. In the latter part of the section, elements of the theory are given with equations and figures for clarification.

Digital modems—long-distance communication channels—use a procedure of (1) sampling the analog input, (2) digitizing it, (3) transmitting it, and then (4) decoding it into analog output at the receiving station. Similarly, digital informa-

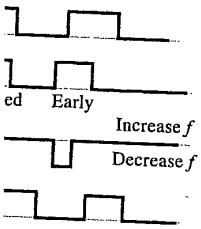

at PLO module.

ad-back clock is in synchronization
he codes have embedded the clock
es that periodic pulses will appear.
compared with the standard clock
s between the two are corrected by
corresponding detection windows.
the data timing correction. Differ-
data timings are registered, and a
ie phase-locked loop now modifies
ect of the required correction. The
a pulse timings according to short
clock frequency responds only to
to data intervals take place on a

nunication field. The term PRML
onse and ML for maximum like-
(1, 7) with sampling and maxi-
ses the principle of this concept.
tions of using a PRML channel.
long with a comparison between
rt of the section, elements of the
rification.
ion channels—use a procedure
(3) transmitting it, and then (4)
tion. Similarly, digital informa-

tion is converted by the writing head to an analog input to the disk, which is later read as an analog output to the read detection channel. The PRML channel takes the analog output signal from the reading preamplifier, filters it (or equalizes it) to shape it appropriately, samples it, and then uses a procedure to detect the signal with high reliability.

The advantages of the sampled detection in a noisy environment have been well known in data communications. The applications of these procedures to the disk drive industry came into focus in the early 1970s with publication of several papers from IBM researchers. The subject took on a new importance with announcements of drives with PRML channels in 1989. Note that the first product (IBM 0681 in 1990) using PRML employed MIG heads. Application of PRML is not synonymous with the use of MR heads.

8.13.1 Motivation

The motivating factors leading to conversion of the recording channel in disk drives from peak detection to PRML are summarized as follows:

1. Researchers working on sampled detection (PRML) channels modeled and experimentally verified that a PRML channel can give 20–30% additional linear density compared to a peak detect (1, 7) channel with identical components (head, medium) and flying heights.
2. The move to PRML entails a digitization of the channel. The use of digital servo and digital controls of the spindle along with a digital channel have many advantages. Powerful digital signal processing techniques developed in other fields can be applied to disk drives. Use of digital components results in miniaturization and standardization of LSI (large-scale integration) circuitry along with a lower power requirement and lower cost.
3. The digital channel lends itself to self-diagnosis, leading to higher yields in manufacturing and potential convenience during maintenance of the device. Special test patterns are used that, when examined after sampling of data, allow medium surface monitoring and give insight into the variability of flying heights and potential for failures.
4. In the process of peak detection, the signal is differentiated for generating zero cross-over. This process amplifies higher frequencies, which in turn contributes additional noise and increased errors. The sampling process measures amplitudes at specific intervals and eliminates this step.

8.13.2 Explanation of PRML and Comparison with Peak Detection Channel

The words *pulse, signal, symbol,* and *transition* are used interchangeably in this discussion. Figure 8.16 shows the superposed data pulses as they would occur at a high linear density of flux transitions in peak detect procedure. Peaks of the pulses are detected within allocated windows. The most pulse crowding possible with peak detect is shown in this figure. Figure 8.17 indicates two consecutive pulses of a

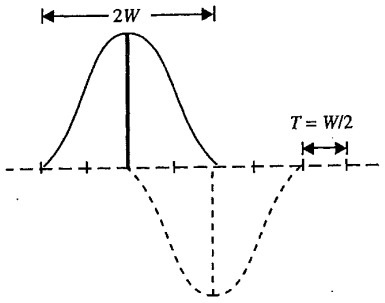

Figure 8.16 Peak detection.

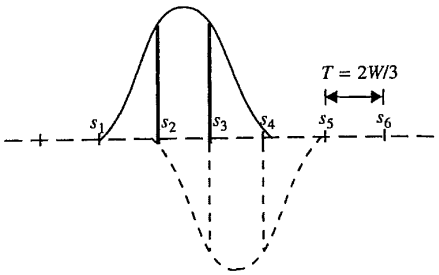

Figure 8.17 PRML sampling.

PRML channel. At every clock time T distance apart, samples of the signal voltage are taken. The W in the figure is a half pulse width. For now, let us consider a single pulse, as shown by a solid line in Figure 8.17.

At positions s_1, s_2, s_3, and s_4, the sampled outcomes are 0, 1, 1, and 0, respectively. Sampling at the two positions s_2 and s_3 for the pulse gives nonzero outcomes, while sampling at s_1 and s_4 always gives zeros. For a variety of PRML channels, this type of sampling channel, with two nonzero sampling locations per pulse, is called a *partial response channel of class IV.* Now consider both adjacent pulses (solid and dashed lines) in Figure 8.17. Two pulse waveforms are *allowed* to superpose but in prescribed positions. The second (negative) pulse is a displaced image of the first pulse. The displacement is time T. Every additional pulse (not shown) in a sequence of pulses will be similarly displaced by exactly one sample position T apart. When sampled voltages of the two pulses are measured at s_1, s_2, s_3, s_4, and s_5 and digitized, the result is the sequence 0, 1, 0, −1, and 0. Note that there are three levels to be detected for this sampling channel, compared to only two (+1, −1) for the peak detect channel. The pulse waveform for PRML channels should have a certain shape and frequency relationship. Special filters are developed for this purpose, and this topic is described in the next section. Higher overlap of adjacent pulses is possible with partial response channels, as seen in Figure 8.17.

The second part of PRML, that is, maximum likelihood, is also discussed in Section 8.13.4. We simply state the idea here. In the case of a peak detect procedure every pulse is treated and detected independently without using any information from the adjacent pulses or data already read. In the maximum likelihood case, several pulses or symbols are treated as an entity and detected simultaneously. Not only is a sequence of pulses treated together, but a sliding window of a sequence of pulses is detected simultaneously in a continuous manner. For a detection of every sequence, questions are asked regarding which of the possible outcomes is most likely for the sequence being detected based on the statistical inference of the prior information. This provides a minimum error possibility or maximum likelihood detection.

One objective of the PRML channel is to increase linear bit density. A figure of merit has been devised to compare the density capabilities of a variety

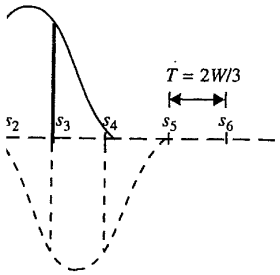

L sampling.

:t, samples of the signal voltage
For now, let us consider a single

:omes are 0, 1, 1, and 0, respec-
: pulse gives nonzero outcomes,
r a variety of PRML channels,
ampling locations per pulse, is
consider both adjacent pulses
aveforms are *allowed* to super-
ive) pulse is a displaced image
additional pulse (not shown) in
exactly one sample position *T*
neasured at s_1, s_2, s_3, s_4, and s_5
and 0. Note that there are three
mpared to only two (+1, −1)
r PRML channels should have
l filters are developed for this
on. Higher overlap of adjacent
seen in Figure 8.17.
likelihood, is also discussed in
:ase of a peak detect procedure,
ıout using any information from
imum likelihood case, several
d simultaneously. Not only is a
ıdow of a sequence of pulses is
a detection of every sequence,
outcomes is most likely for the
rence of the prior information.
num likelihood detection.
:ease linear bit density. A fig-
ısity capabilities of a variety

of channels. A magnetic transition is read as a pulse. The function of the channel and coding is to give the maximum number of customer bits per pulse width. The figure of merit is defined as the number of customer or user bits per half pulse width (P_{50}) at the preamplifier output.

To compare the figure of merits for peak detect and a PRML channel, consider an idealized Lorentzian pulse waveform and no filtering. For those unfamiliar with the concept of resolution as applied to the linear density of a disk drive, a review of Section 8.18 could be helpful here. As the density increases, interference between pulses increases and peak voltages of the pulses drop. For the (1, 7) peak detection procedure, a resolution of 50% (which means a drop in voltage to half its peak value) is considered detectable. Equation (8.16), derived for Lorentzian pulse shapes, indicates that spacing between peaks of adjacent pulses will be a certain fraction (1.39) of half-voltage pulse width (P_{50}). This also means that the highest density of 1.39 peak spacing for a given pulse width of signal pulse is allowable for reliable detection of a signal for a peak detect channel. For this example, we assume a half pulse width, *W*, to be the same as P_{50} where signal drops from peak to 50% signal value. To convert coded bits to customer bits, the multiplier for (1, 7) peak detect channel is $\frac{4}{3}$. So to find customer bits per half pulse width we get $\frac{4}{3} \times 1.39$, which yields 1.85. Practical numbers range between 1.5 and 1.7 bits per nonfiltered half pulse width. A PRML channel can operate at a very low resolution and still be effective in providing data extraction with an acceptably low error rate. The process of combining sampling and maximum likelihood detection provides this advantage to PRML. The total density of practical PRML channels range between 2 and 2.5 user bits per half pulse width. Table 8.2 summarizes differences between peak detection and the PRML channel.

8.13.3 Partial Response

Elements of PRML theory are addressed next. First, consider the principle of partial response (PR). Figure 8.18a shows a signal pulse resulting from reading a transition in the media.

A sampling procedure to detect the signal is to sample the amplitude of the signal at regular intervals of time *T* apart, as shown. When the sampling circuit shows an amplitude larger than the predefined value (threshold), existence of the '1' is realized. This procedure can be improved if the signal is equalized or filtered so that the resultant pulse to be detected is such that it has nonzero value at only one sampled time and at all other sampled times it is zero. Such an equalizer can be designed. Figure 8.18c shows a filtered output with nonzero output at a single sampled time. At all other sampling times output is ideally zero. This type of filter and channel are called "full-response" filter and "full-response" channel. The frequency boost required for such a filter is quite high and adds significant noise to the output.

A modified sampling procedure has been devised that provides a more balanced approach in the trade-off between addition of noise by high-frequency boost versus intersymbol elimination. Two sampled locations may have nonzero amplitudes corresponding to a single pulse but the response at other sampled times will be

TABLE 8.2 Comparison of Peak Detect and PRML Channels

Peak Detect Channel (1, 7)	PRML Channel
Signal peaks are detected within the time window.	Signal values are registered at sampled times.
One pulse is detected at a time to determine if the output is 1 or 0.	A series of samples are taken at regular time intervals for a set of pulses, and signal values are extracted for the sequence by using a statistical maximum likelihood process.
Signals are slimmed (equalized) to reduce ISI. Slimming adds high-frequency content and noise to the signal.	Adjacent pulses are allowed to overlap with a provision that sampling times coincide for overlapping pulses. Precise filtering is needed to shape the pulses, which add to signal noise.
Differentiation of the pulse to detect zero crossing within the window adds noise to the signal.	No signal differentiation is required.
Signal-to-noise ratio needs to be high to detect a signal from interference and noise.	The sampled signal detection process allows for a lower (1.5–3-dB) signal-to-noise ratio for the same error rates.
Two states (0, 1) are required.	Sample values have three states for the PRML channel (+1, 0, −1).
The need for high signal-to-noise ratio for an acceptable error rate requires that the highest flux changes allowable are limited to about 50% resolution.	PRML sampling and detection procedures allow successful detection (acceptable error rate) at a flux change density resolution of between 10 and 30%.
The half pulse width accommodates up to 1.7 user bits.	The half pulse width of the signal may accommodate between 2 and 2.5 customer bits.
Little if any dramatic extensions of pure peak detect processes are likely in the foreseeable future.	Progress in the PRML channel depends on data communication and integrated circuit technologies, both of which are heavily explored. Chances of extending the disk drive capabilities through PRML are high as these technologies progress.

zero. Figure 8.19c shows such a modified pulse form. Such a signal is called a *partial response signal,* and a channel that uses such signals is called a *partial response channel of class IV.* The filter that results in such a signal output for an isolated transition signal is called a *class IV partial response filter,* or *PR-IV filter* (Figure 8.19b) for short. Repeating the characteristic of a partial response signal here, it has nonzero values at $t = 0$ and $t = T$ but zero at all other sampled times. It is useful to describe a PR pulse waveform mathematically that satisfies the above criteria. It turns out that there are many waveforms that can meet the criteria. Impo-

PRML Channel
lues are registered at sampled times.
of samples are taken at regular time for a set of pulses, and signal values are for the sequence by using a statistical likelihood process.
pulses are allowed to overlap with n that sampling times coincide for ig pulses. Precise filtering is needed to pulses, which add to signal noise.
differentiation is required.
ed signal detection process allows for .5–3-dB) signal-to-noise ratio for the rates.
lues have three states for the PRML -1, 0, −1).
npling and detection procedures allow detection (acceptable error rate) at a e density resolution of between 10 and
ulse width of the signal may ate between 2 and 2.5 customer
the PRML channel depends on unication and integrated circuit s, both of which are heavily explored. extending the disk drive capabilities ML are high as these technologies

se form. Such a signal is called a
es such signals is called a *partial*
ults in such a signal output for an
tial response filter, or *PR-IV filter*
eristic of a partial response signal
ut zero at all other sampled times.
nematically that satisfies the above
ns that can meet the criteria. Impo-

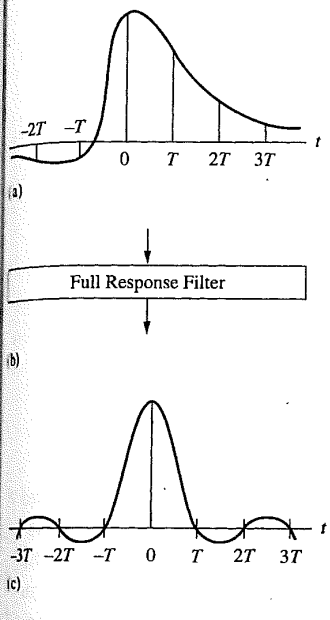

Figure 8.18 (a) Signal pulse before filtering; (b) full response filtering; and (c) full response filtered signal.

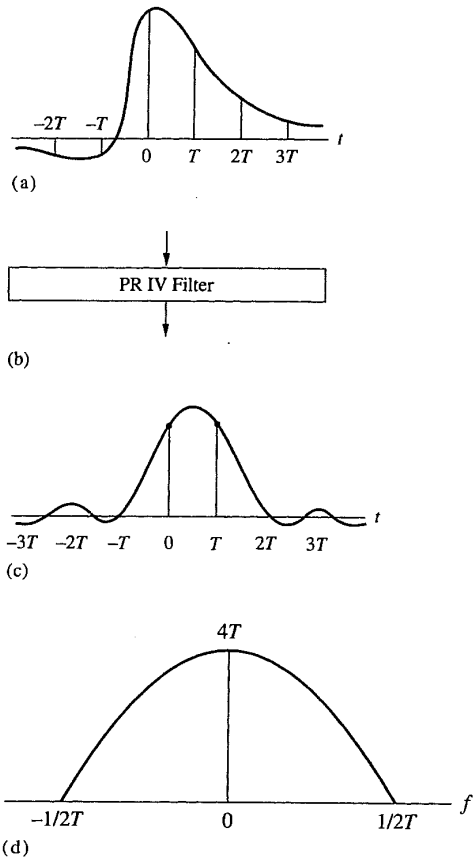

Figure 8.19 (a) Signal pulse before filtering; (b) partial response (IV) filtering; (c) ideal partial response filtered signal; and (d) frequency response of PR-IV filter.

sition of an additional constraint that the waveform must have minimum frequency bandwidth results in a unique solution given by

$$V(t) = 2\left\{\frac{\sin(\pi t/T)}{\pi t/T} + \frac{\sin[\pi(t-T)/T]}{\pi(t-T)/T}\right\} \tag{8.8}$$

Figure 8.19c shows this time function. The frequency domain or Fourier transform magnitude of the signal is given by

$$4T\cos(\pi f T), \text{ with } |f| < \frac{1}{2T} \tag{8.9}$$

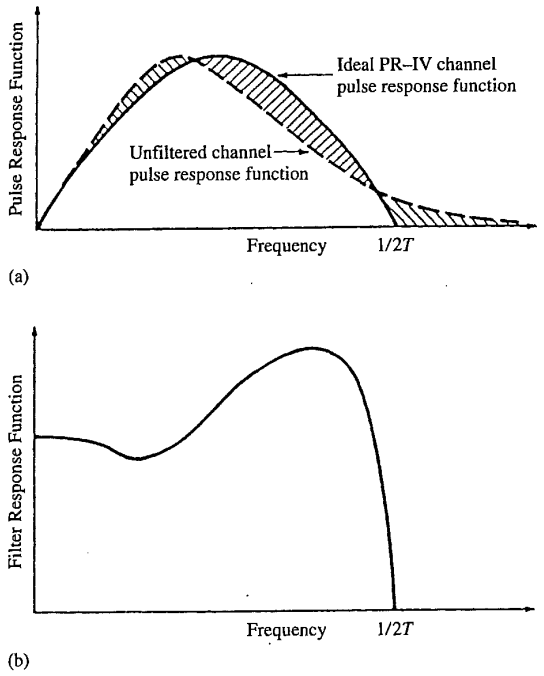

Figure 8.20 (a) Unfiltered and PR-IV filtered frequency response; (b) PR-IV frequency filter characteristic.

Figure 8.19d shows this frequency characteristic. Figure 8.20a shows an unfiltered channel pulse response function. Also shown is the ideal PR-IV response function that can result as the signal output of Figure 8.19c. It is required that the multiplication of an unfiltered channel response and the filter response function in frequency domain should result in a desired ideal PR-IV pulse response function. Figure 8.20b qualitatively indicates such a filter response function. Note the high-frequency boost and sharp cutoff frequency of the response function.

Summarizing, partial response is a sampling procedure used to detect signals after they are conditioned by a filter (or equalizer) so that intersymbol interference is less detrimental and the signal-to-noise ratio is enhanced. Digitization of the channel has several advantages in addition to the increase in linear density.

8.13.4 Maximum Likelihood

In the case of a peak detection process, every bit is individually detected. In the digital communication field, a different method became popular in which a detected sequence of bits is looked at as a unit and the question is asked, "out of a number of possible original data bit sequences, which one is most likely to result in the observed sequence?" This can most aptly be reworded as "having the highest probability." A more mathematical way to define the procedure is to reduce the

al PR–IV channel
se response function

quency response; (b) PR-IV

igure 8.20a shows an unfiltered
he ideal PR-IV response func-
e 8.19c. It is required that the
nd the filter response function
al PR-IV pulse response func-
ter response function. Note the
the response function.
rocedure used to detect signals
that intersymbol interference is
nced. Digitization of the chan-
e in linear density.

y bit is individually detected.
od became popular in which a
he question is asked, "out of a
ch one is most likely to result
reworded as "having the high-
the procedure is to reduce the

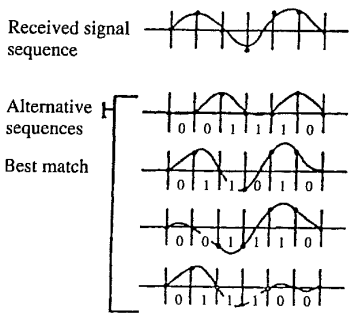

Figure 8.21 Maximum likelihood sequence detection.

mean-square error between detected data sequence and one of the several optional sequences that might cause such an output. Figure 8.21 shows a situation in which a sequence of bits is detected and compared with possible "close" sequences that could have produced the resultant sequence. The figure is an ideal representation of the output. In reality, noise and distortion will be present in the sequence. It would be laborious and impossible to compare the observed sequence of data with every conceivable input sequence within a reasonable time. However, algorithms were developed in the late 1960s for solving such error minimization problems [5]. Maximum likelihood codes for disk drive application use these algorithms.

In case of PRML, 8 user bits are converted into 9 coded bits; hence, its code rate is 8/9. Sampling is a distinctly different procedure to peak detection process. However, for comparison, peak detection terminology is often used. In Table 8.1, detection window time and other parameters are calculated as shown. No logical criterion for high- to low-frequency ratio is known, but as an analogy to (1, 7) peak detect channel, a value of 4 is customarily used. A minimum number of zeros between 1's can be 0 for PRML channel, while a maximum of 4 zeros are allowed for every odd and even sequence. This constraint comes from the use of Viterbi maximum likelihood algorithms employed for PRML detection procedure.

8.14 EXTENDED PRML AND (1, 7) MAXIMUM LIKELIHOOD CHANNELS

The PRML channel allows overlapping of the pulses, as seen in Figure 8.17. It is natural to inquire if further overlapping of pulses can be attempted. The answer is yes. Figure 8.22a shows two pulses that overlap to a larger extent than those in Figure 8.17. The sampling time interval is shortened, and more samples per pulse waveform are now taken.

Note that there are two levels of nonzero pulses compared to the PRML case. The smaller and larger amplitudes detected during sampling are designated level 1

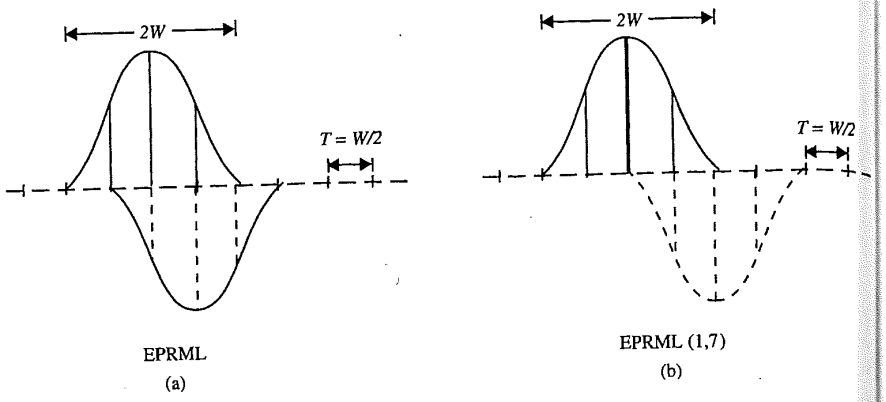

Figure 8.22 EPRML and EPRML (1, 7) signal sampling [6].

and level 2. So the sampling process here results in five levels: $-2, -1, 0, +1$, and $+2$. This type of channel is called EPRML, for extended partial response channel. There are four sampling periods within a pulse; hence, each period is one-fourth of the pulse width. The penalty in using EPRML is the increased complexity of working with five-level logic and more involved semiconductor circuits. A combination of (1, 7) coding along with EPRML-style sampling has been described [6]. The capacity of the channel for this case is the same as the PRML channel; however, the merits of the method are the constraint of a 0 between two 1's, which results in more stable sampling times; no notch filtering; and robust, less error-prone detection. Another advantage of this channel is that it avoids the severe high-frequency boost and notch of the often troublesome PRML channel filter. This channel has been used in the IBM 3390-9 drive.

8.15 MAGNETIC RECORDING MEASUREMENTS OF WRITE AND READ PARAMETERS

Often technical concepts are best realized through understanding of measurement procedures. The disk drive recording measurements most commonly carried out to characterize heads and disks are described next. Traditionally, testing and evaluation of linear density is carried out in a setup known as a *magnetic recording test* while integration of linear density and track density parameters are done on precision test stands (PTSs). Both procedures attempt to simulate various elements of a head-disk assembly (HDA) for design and diagnostics of components. Magnetic recording testers commonly use ball-bearing spindles for disk mounting and motor-driven screw-type actuators to move the head across the disk radially. Precision testers have air-bearing spindles and laser interferometer-controlled head movement.

Another factor that separates these two test setups is the degree of stability required. The PTS is used to measure very small off-track head movements and the results must be accurately repeatable; hence, these stands require heavy granite bases and precise environmental controls. With reduced disk sizes, reduced cost of the air-bearing spindles for small disks and modular approaches to measuring instruments, the distinction between the two types of testing be-

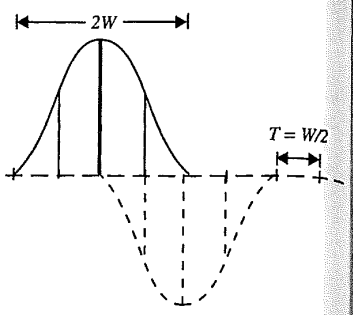

EPRML (1,7)

(b)

ɪnal sampling [6].

in five levels: −2, −1, 0, +1, and
extended partial response channel.
hence, each period is one-fourth of
the increased complexity of work-
iconductor circuits. A combination
ɔling has been described [6]. The
ɛ as the PRML channel; however,
l between two 1's, which results in
and robust, less error-prone detec-
: avoids the severe high-frequency
L channel filter. This channel has

S

hrough understanding of measure-
ɪurements most commonly carried
ext. Traditionally, testing and eval-
ɪown as a *magnetic recording test*,
ty parameters are done on precision
ɪulate various elements of a head-
ɪ of components. Magnetic record-
ɔr disk mounting and motor-driven
lisk radially. Precision testers have
trolled head movement.
ɛst setups is the degree of stabil-
small off-track head movements,
ɪence, these stands require heavy
ɔls. With reduced disk sizes, re-
ll disks and modular approaches
een the two types of testing be-

comes blurred, and a single setup is able to handle both functions at a modest cost. Here are a few of the reasons for carrying out magnetic recording measurements.

1. The process of *overwrite measurement* is to measure the remnant of the old signal after the new signal is written over it. The overwrite specification ensures that the new signal is free of old data for error-free detection during reading. This parameter is influenced by several factors:
   (a) Head writability, which depends on head current, head pole material, and head pole design
   (b) Medium coercivity, remanence magnetization, and thickness

   The disk drive writing process is highly nonlinear and complex. No simple analytical or numerical methods are satisfactory; hence, an experimental procedure is necessary. Measurement of overwrite as a function of head and medium parameters gives good insight into the design and diagnostics of read/write components and electronics. The measurement is described in Section 8.16.
2. Establishment of adequate write current. The write current must be high enough so that overwrite is sufficiently high. The current must saturate the medium for even signal magnitudes. The transition parameter a depends on the write current rise time. Too large a write current may widen written track widths and affect track density of the disk drive. Section 8.17 discusses write current measurement and its influence on these design parameters.
3. Measurements of roll-off and resolution parameters. These measurements are directly related to linear bit density; hence, they are used to establish specifications of linear bit density, select head-disk parameters, and verify design during the development cycle. The measurements also provide feedback during optimization of write electronics, filter design, and detection of circuit components.
4. Measurements of signals and noise to establish the dependence of signal-to-noise ratio for different operating conditions.

Often, additional recording measurements are tailored for specific heads and disks. For example, narrow-track thin film heads are prone to domain-related instabilities; hence, some procedure to measure this tendency is required. The MR heads are subject to uneven signal magnitudes in up-versus-down directions (asymmetry), and measurements are tailored to investigate that on a PTS.

8.16 OVERWRITE AND ITS MEASUREMENTS

The procedure of "writing" on a disk track has two functions:

1. To erase previously written information.
2. To write new data.

In principle, these functions can be performed as two separate steps. However, separate steps require twice the latency time and add to the write access time. The process of overwriting or performing these functions in one step is not new to magnetic recording. Audio recorders and digital recorders operate in a combined overwrite process. Efficacy of the write process is measured by the degree of eraseability of old data when new information is written.

From the first principles of the Fourier series, it is known that a single digital pulse consists of harmonics or a series of frequencies. Also a sequence of digital data consists of a range of frequencies. When this data is written on a magnetic track, it is equivalent to writing a band of sinusoidal frequencies. When there are many 0's compared to 1's in a stream of data, low frequencies dominate, while a large concentration of 1's in data results in more of the higher frequencies.

It is known experimentally that it is most difficult to write high-frequency data on top of prior low-frequency data. To ensure error-free data, a criterion is set for overwrite measurement that is "conservative" and simulates the condition of writing with high frequency on top of low frequency.

When a pattern of low frequency, all 1's, is written on a clean track and the track is read back displaying output on a spectrum analyzer, a line corresponding to the recorded low frequency will be seen on a frequency-versus-voltage plot. Figure 8.23 shows a plot of such responses for a range of frequencies and corresponding voltage outputs. Each of these frequencies is written with the same write current. Notice that the voltage outputs start dropping at higher frequencies. For the overwrite measurement only two of these frequencies are considered. We call these frequencies f_l for lower frequency and f_h for higher frequency. These frequencies, for different codes, are discussed in Section 8.6. The procedure for the measurement of overwrite is as follows:

8.17

1. Select a track to write on and DC erase it, which means passing a high DC current through the head coil while the disk track rotates under the head. This process removes any prior data from the track.
2. Write a low-frequency f_l, all 1's, signal on the track and measure voltage V_l (Figure 8.23).
3. Without erasing the track, superimpose writing with a high-frequency f_h pattern of 1's with the same current level as used for writing low frequency.
4. Measure leftover low-frequency V_a.

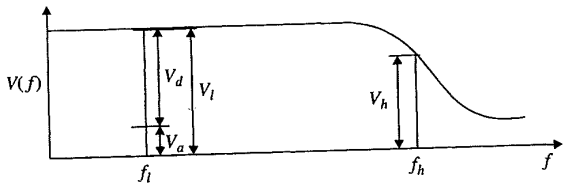

Figure 8.23 Overwrite definition and measurement.

as two separate steps. However,
ld to the write access time. The
s in one step is not new to mag-
ers operate in a combined over-
red by the degree of eraseability

it is known that a single digital
ies. Also a sequence of digital
; data is written on a magnetic
al frequencies. When there are
frequencies dominate, while a
the higher frequencies.
fficult to write high-frequency
error-free data, a criterion is set
and simulates the condition of
y.
vritten on a clean track and the
nalyzer, a line corresponding to
ncy-versus-voltage plot. Figure
frequencies and corresponding
en with the same write current.
gher frequencies. For the over-
e considered. We call these fre-
equency. These frequencies, for
procedure for the measurement

which means passing a high DC
sk track rotates under the head.
the track.
n the track and measure voltage

riting with a high-frequency f_h
used for writing low frequency.

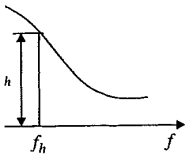

l measurement.

The overwrite is now defined as

$$\text{Overwrite (dB)} = 20 \log\left(\frac{V_a}{V_l}\right) \tag{8.10}$$

Since V_a is always smaller than V_l, the quantity is measured in negative numbers. Overwrite of -30 dB and smaller is considered good, while that of less than -25 dB will be unacceptable for a commercial drive. Sometimes the overwrite is expressed as a percentage of $100 \times (V_l - V_a)/V_l$. In this form, this quantity is referred to as *write-over loss.*

In the section on coding (Section 8.6), high and low frequencies for specific codes are described. For a (1, 7) code the ratio of f_h/f_l is 4. The high-frequency f_h is half the highest flux transition rate written on the disk. Two magnetic flux transitions result in one cycle.

As an example, let us consider the linear density of flux changes or flux transitions on the disk as 2000 fc/mm at the inner diameter of the disk. Let the linear velocity of the disk at the inner diameter be 10 m/s, or 10,000 mm/s. The flux transition rate is then 20 million per second. The maximum frequency of 10 MHz and low frequency of 2.5 MHz would be applicable for the (1, 7) coded data pattern.

Overwrite measurements are performed at several diameters of the disk. Generally, overwrite is weakest at the outer diameter since the head flying height is maximum there.

8.17 WRITE CURRENT OPTIMIZATION FOR RECORDING

The determination of a proper write current is an important step in the design and integration of a disk drive. The following considerations are involved in determining the appropriate value of the write current:

- The write current must be sufficiently large to saturate the medium during the writing process.
- Also, it should be large so as to achieve acceptable overwrite, as discussed in Section 8.16. Erasure of previous data on the track is necessary to reduce error rates.
- Too large a write current results in bit shifts, as discussed in Section 3.12.
- The write current also influences the erase bands at the boundaries of the track width. Large currents increase the erased track width and increase interference between adjacent tracks.

We saw in Chapter 3 that a short-transition parameter a is desirable for high peak-to-peak voltage. Detailed write analyses indicate that there is an optimum current when the slope of the H field is maximum and results in shortest a. The process of

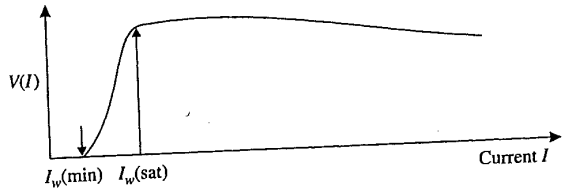

Figure 8.24 Write current optimization.

writing involves partial saturation of the head poles and a nonlinear **B–H** loop (Section 2.13) of the medium. The complexity of the processes precludes easy analytical or numerical determination of the optimum write current. Experimental procedures are heavily relied on for this purpose. Experiments are carried out by varying write currents and observing several parameters. Figure 8.24 shows a plot of peak-to-peak voltage read from a track (usually at the inner diameter of the disk) as a function of changing write currents. For small currents the medium does not saturate, and the signal output is low. As the write current increases, at some value the signal voltage is maximum, and further increase in current does not add to the voltage significantly. The current I_w (sat) or a slightly higher current is a good choice for further testing and possibly for use in the drive, provided high overwrite is also obtained at that current. Several additional tests may be carried out prior to the selection of the write current.

Figure 8.25 shows overwrite as a function of the write current. Overwrite increases with current, and after some point further increase in current does not add to the overwrite due to head saturation. These experiments are carried out at the inner and outer diameters of the disk. At the outer diameter the flying height is higher, and hence overwrite tends to be lower than that at the inner diameter of the disk. The required current to provide sufficient overwrite throughout the surface of the disk is evaluated. Since there are penalties for too large a write current, it is ensured that once the voltage signal is close to the highest level and overwrite is better than the specified value (in the range of −25 to −35 dB), the write current is restrained to the smallest possible value.

8.18

The topic of fringing fields and erase bands has been discussed in Section 3.13, and the effect of overlapping tracks is considered in Section 9.11. These fringing fields can produce crosstalk in adjacent tracks and erase part of the adjacent tracks.

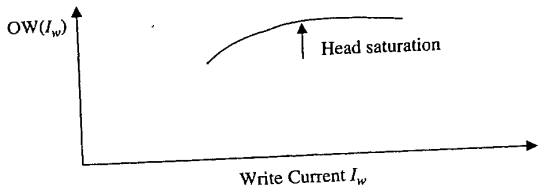

Figure 8.25 Overwrite as a function of write current.

Current I

optimization.

ɔles and a nonlinear **B–H** loop (Sec-
processes precludes easy analytical
:e current. Experimental procedures
:nts are carried out by varying write
re 8.24 shows a plot of peak-to-peak
iameter of the disk) as a function of
medium does not saturate, and the
ɜes, at some value the signal voltage
s not add to the voltage significantly.
is a good choice for further testing
h overwrite is also obtained at that
out prior to the selection of the write

on of the write current. Overwrite
urther increase in current does not
ıese experiments are carried out at
ɛ outer diameter the flying height is
han that at the inner diameter of the
overwrite throughout the surface of
ɜ for too large a write current, it is
› the highest level and overwrite is
−25 to −35 dB), the write current

ɜ has been discussed in Section 3.13,
red in Section 9.11. These fringing
ınd erase part of the adjacent tracks.

lead saturation

ıt I_w

ion of write current.

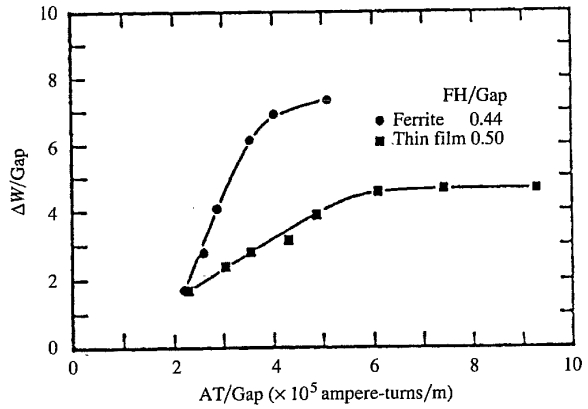

Figure 8.26 Track width widening versus ampere-turns per meter for ferrite and film heads [7].

Figure 8.26 shows the results of an experimental study to relate increased track width with increased coil ampere-turns [7]. Here it suffices to indicate that increasing the write current produces increased fringing fields at the edges of the head pole track widths, and the current is limited to avoid interference among adjacent tracks. Due to the influence of the write current on interactions among several parameters, more detailed studies of the write current versus signal, noise, peak shift, and error rates are often carried out to optimize the disk drive density.

8.18 LINEAR DENSITY ROLL-OFF CURVE AND RESOLUTION

In Section 8.3, the concept of intersymbol interference and consequent decrease in voltage as a function of increasing magnetization flux changes has been described. The graphical plot of flux change density versus signal voltage is called the *roll-off curve*. To plot the roll-off curve, a series pattern of 1111 ··· is written throughout the track of a disk at an optimized current, discussed in the last section. The sequence is now read, and the zero-to-peak voltage is measured. The process is repeated with higher density of the same pattern until a signal becomes too small. The curve is plotted with the x axis as the number of flux changes per millimeter and output voltage on the y axis. More often, though, the voltage readings are normalized by a low-frequency voltage value.

Figure 8.27 illustrates a roll-off plot. The roll-off curve is used to define the term resolution of the system. Corresponding to the low frequency (f_l) and high frequency (f_h) used for overwrite, low and high flux changes per millimeter are used to define resolution. From the plot, voltages V_l and V_h for low and high flux changes per millimeter are obtained. The "resolution" is the voltage ratio in percentage: $100 \times V_h/V_l$. For the (1, 7) peak detect channel and where resolution drops to 50%,

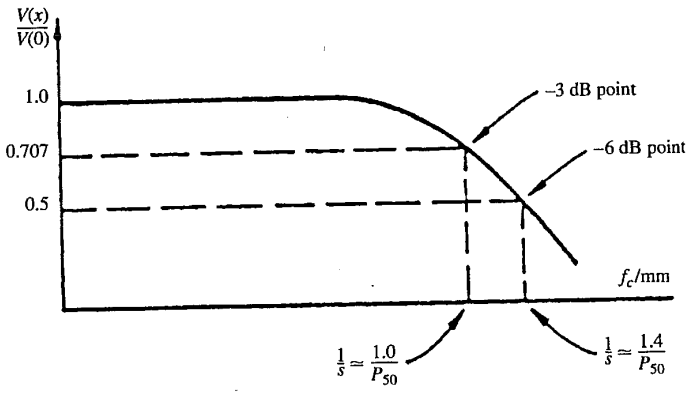

Figure 8.27 Roll-off curve of a Lorentzian pulse.

the flux change per millimeter is commonly quoted as an acceptable density. In the case of large disk drives with a (2, 7) peak detect channel and thin film and thin pole ($\approx$1 μm) heads, conservatively 70% and above resolutions were used. The required resolution defines the highest flux change per millimeter (or corresponding bits per inch) usable for the system. If the coding and detection are highly efficient, it is possible to operate the system at very low resolution along with low acceptable error rates. The PRML and EPRML are such channels and are discussed in Sections 8.13 and 8.14. The channel modeling to predict the resolution and highest density is useful in projecting future products. Usually these models are hybrids of mathematical equations and experimentally collected data. As a learning tool it is instructive to calculate resolution versus flux changes per millimeter for a simple pulse waveform. The procedure provides insight into the methods used for more complex models.

Let us assume that the voltage output of an isolated single transition is given by a pulse form known as a Lorentzian pulse (also discussed in Section 3.11):

$$V(x) = \frac{V(0)}{1 + (2x/P_{50})^2} \tag{8.11}$$

Figure 8.28 shows such a pulse. Note that at $x = 0$ the pulse has a peak value $V(0)$ and at $x = \pm P_{50}/2$, the pulse amplitude is one-half of the maximum, which is the definition of P_{50}. The question we want to answer is: "What happens to the magnitude of peak voltage when the foregoing pulse is gradually crowded by similar positive and negative pulses along the x axis from $-\infty$ to $+\infty$?" We discussed the reduction in signal due to pulse crowding in Section 8.3 on intersymbol interference. It is possible to describe this problem by an equation assuming linear superposition of pulses as

$$V(x, s) = \sum_{n=-\infty}^{\infty} (-1)^n \frac{V(0)}{1 + (2x + 2ns/P_{50})^2} \tag{8.12}$$

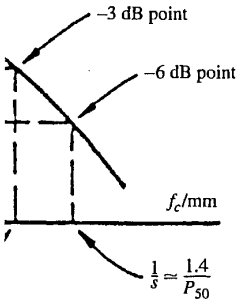

tzian pulse.

ıs an acceptable density. In the
:hannel and thin film and thin
/e resolutions were used. The
:r millimeter (or corresponding
l detection are highly efficient,
lution along with low accept-
:hannels and are discussed in
dict the resolution and highest
ly these models are hybrids of
d data. As a learning tool it is
:s per millimeter for a simple
to the methods used for more

ated single transition is given
scussed in Section 3.11):

(8.11)

ıe pulse has a peak value $V(0)$
)f the maximum, which is the
:: "What happens to the mag-
gradually crowded by similar
to $+\infty$?" We discussed the re-
) on intersymbol interference.
assuming linear superposition

$$\frac{)}{2ns/P_{50})^2} \qquad (8.12)$$

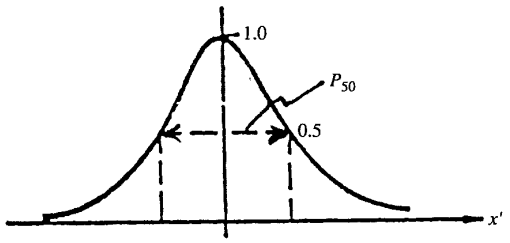

Figure 8.28 Lorentzian pulse.

where s is the spacing between peaks of consecutive pulses. Different values of n correspond to the same voltage pulse displaced by spacings given by ns. The expression (8.12) sums all these pulses for a given spacing s. This series has an explicit solution [8]:

$$V(x, s) = V(0)k\frac{\sinh(k)\cos(\pi x/s)}{\cosh^2 k - \cos^2(\pi x/s)} \qquad (8.13)$$

where $k = \pi P_{50}/2s$. We are only interested in the value of the signal amplitude for the pulse peak at $x = 0$; hence, substituting $x = 0$ in equation (8.13),

$$V(0, s) = V(0)\frac{k}{\sinh(k)} \qquad (8.14)$$

$V(0, s)$ is the reduced voltage due to crowding of pulses spaced s apart. At large spacings (as s approaches ∞), $V(0, s)$ approaches $V(0)$, the peak amplitude of the isolated pulse. Using this equation, the value of voltage at any spacing can be found. Asking the reverse question—"What is the spacing at which peak voltage is reduced by one-half (or -6 dB)?"—the solution is obtained from

$$\frac{V(0)}{2} = V(0)\frac{k}{\sinh k} \qquad (8.15)$$

by trial and error or plotting and gives

$$s = \frac{P_{50}}{1.39} \qquad (8.16)$$

Along the lines of the foregoing procedure, the spacing s can be determined when voltage reduces to -3 dB, or 0.707 of the original peak value, which is a criterion often used in drive design. It is simply $s = P_{50}$. If P_{50} and s are given in nanometers, the flux change that is the reciprocal of spacing is given by fc/mm $= 1/s \times 10^6$. Resolution points 0.707 and 0.5 are indicated in Figure 8.27.

If the actual pulse cannot be expressed by a Lorentzian pulse, an experimental voltage pulse can be used for higher accuracy. The procedure then would be to sum up a series of experimental pulse voltages on a computer and reduce the spacing,

step by step, to calculate a series of voltage values. The spacings at which voltage reduces to a predetermined value can also be derived. Practically only a few (four to eight) pulses need to be summed for the procedure. An analytical voltage waveform or experimental pulse converted into analytical form can also be similarly used.

8.19 NOISE SOURCES IN RECORDING PROCESSES

A crucial topic in the transmission and storage of electronic information is noise. It is important in consumer electronics, the communication of data, and almost all fields of electronics where an accurate signal is to be extracted from an inevitably noisy environment. Much of the research in understanding noise sources, coding schemes to transmit data with low error rates, and error correction procedures was initiated in the telephone industry.

In the case of disk storage, the signal is relatively small, that is, less than a millivolt, while additive noises and perturbations can make detection of data difficult or result in unacceptable errors. A commonly recognized figure of merit in the industry is the signal-to-noise ratio. A higher signal-to-noise ratio results in a more robust drive. A historical fact is that the signal-to-noise ratio and the size of a signal in disk drives have remained within a short range despite dramatic changes in the technology in the last four decades. The pursuit of higher densities has resulted in increased noise. Higher linear densities require wider bandwidths, which result in increased electronic component noise. Increasing track density results in more interference from adjacent tracks and also makes the signal more susceptible to defects in medium. Major disk storage research involves the development of low-noise components and procedures to reduce interfering disturbances. The next few sections examine the sources of noise and then relate signal to noise quantitatively to the error rate performance of the disk recording system. The sources of noise affecting the performance of a disk drive are listed in Section 8.2 and categorized in Figure 8.29. There are two separate categories of noises in disk drive recording that contribute to error rates. The first—crosstalk noises—are more deterministic and can be reduced with design considerations. The other category consists of "random" noises, and the times of their occurrence are not predictable. Two discussed in this chapter, ISI (Section 8.3) and overwrite (Section 8.16), and two others discussed in Chapter 9, off-track and adjacent-track noises (Sections 9.9 and 9.10), are deterministic-type noises. Here we shall concentrate on the integration of random noises. Electronic noises in heads are quantified in the equivalent circuit in Section 5.7, while medium noise is described in Section 7.4.

An instructive and useful way of looking at the effect of noise on the detection of a recorded signal is shown in Figure 8.30. The signal from an isolated transition is differentiated prior to detection. The zero crossing is expected in the center of the window. A random noise is added to the signal, and the resultant signal now has a zero crossing shifted due to added noise. When noise sources are independent and

uncorre
square r

where I
is the n
noises i

values. The spacings at which voltage
derived. Practically only a few (four
ocedure. An analytical voltage wave-
analytical form can also be similarly

CESSES

ge of electronic information is noise.
ommunication of data, and almost all
is to be extracted from an inevitably
understanding noise sources, coding
, and error correction procedures was

latively small, that is, less than a mil-
can make detection of data difficult or
cognized figure of merit in the indus-
to-noise ratio results in a more robust
se ratio and the size of a signal in disk
pite dramatic changes in the technol-
ier densities has resulted in increased
andwidths, which result in increased
density results in more interference
gnal more susceptible to defects in
the development of low-noise com-
disturbances. The next few sections
gnal to noise quantitatively to the er-
m. The sources of noise affecting the
n 8.2 and categorized in Figure 8.29.
isk drive recording that contribute to
ore deterministic and can be reduced
y consists of "random" noises, and
e. Two discussed in this chapter, ISI
nd two others discussed in Chapter
is 9.9 and 9.10), are deterministic-
integration of random noises. Elec-
ivalent circuit in Section 5.7, while

at the effect of noise on the detection
he signal from an isolated transition
ssing is expected in the center of the
l, and the resultant signal now has
n noise sources are independent and

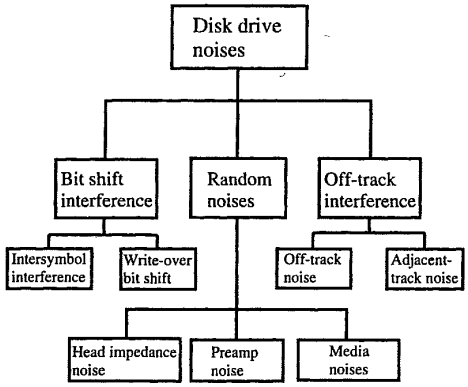

Figure 8.29 Disk drive noises.

uncorrelated, the total random noise voltage E_{nt} can be calculated by finding the square root of the sum of the squares of each random noise as

$$E_{nt} = (E_{nh}^2 + E_{np}^2 + E_{nm}^2)^{1/2} \tag{8.17}$$

where E_{nh} is the head noise voltage, E_{np} is the preamplifier noise voltage, and E_{nm} is the noise voltage due to medium. First, random noise is defined; then random noises in heads, channel preamplifiers, and media are discussed.

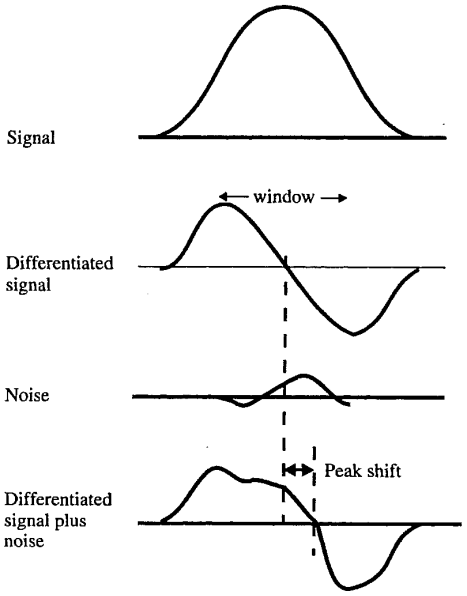

Figure 8.30 Peak shift due to noise.

8.19.1 Random Noise

The fundamental type of noise in electronics is due to the atomicity of matter and electricity. It is completely without regularity in its detailed properties; hence, it is called random noise. However, an average energy of this noise and its frequency distribution is determinable. In 1928, J. B. Johnson showed that minute currents caused by the thermal motion of conduction electrons in a resistor can be detected as a noise source. About the same time, H. Nyquist showed that on the basis of the statistical theory of thermodynamics, thermal noise voltage in an impedance Z is given by

$$E_n = (4kTR\,\Delta f)^{1/2} \tag{8.18}$$

where E_n = rms value of thermal noise voltage
R = resistive component of the impedance in ohms
T = absolute temperature in Kelvin (or degrees Celsius plus 273)
k = Boltzmann's constant = 1.37×10^{23} W-s/deg
Δf = bandwidth of use or measuring system in cycles per second

8.21

For example, 100 Ω resistance at 27°C with a bandwidth of 10 MHz has a thermal noise voltage of approximately 4 μV RMS. It is convenient to express the noise voltage per square root of frequency. So in this case the noise voltage may be expressed as $1.27\text{nV}/\sqrt{\text{Hz}}$. If the resistance component of a circuit is a function of frequency, as it will be for a circuit involving capacitances and inductances besides resistances, equation (8.18) is modified as

$$E_n = \left(4kT \int_0^{\text{BW}} R(f)\delta f\right)^{1/2} \tag{8.19}$$

This equation can be used to calculate head noise voltage if the resistive part of the head impedance varies significantly with the frequency.

Besides the thermal noise, there is another source of random noise called *shot noise*. This was explained by Schottky in 1918 as a variation in current from the hot cathode of a tube amplifier. The finite charge of the electron results in variation of the current and hence contributes as a noise source. The base resistance of a transistor could give rise to significant current variations, or "noise," due to this mechanism.

8.20 HEAD EQUIVALENT CIRCUIT NOISE

In Chapter 5, Section 5.7, an equivalent circuit of an inductive head was discussed. The circuit includes the front-end resistance and capacitance of the preamplifier. The impedance expression from the equivalent circuit is formulated. The real pa

ıics is due to the atomicity of matter
ity in its detailed properties; hence,
nergy of this noise and its frequency

ınson showed that minute currents
ctrons in a resistor can be detected
uist showed that on the basis of the
ıoise voltage in an impedance Z is

$$)^{1/2} \qquad (8.18)$$

ıge
dance in ohms
(or degrees Celsius plus 273)
10^{23} W-s/deg
ystem in cycles per second

ındwidth of 10 MHz has a thermal
s convenient to express the noise
case the noise voltage may be ex-
onent of a circuit is a function of
acitances and inductances besides

$$\delta f\Big)^{1/2} \qquad (8.19)$$

voltage if the resistive part of the
uency.
ource of random noise called *shot*
ıs a variation in current from the
of the electron results in variation
source. The base resistance of a
ariations, or "noise," due to this

ın inductive head was discussed.
capacitance of the preamplifier.
cuit is formulated. The real part

of this impedance is the equivalent resistance of the head (including the preamplifier). This resistance is a function of frequency. The noise voltage of the head can be computed from the integration in equation (8.19). In the case of high damping resistance, the equivalent resistance R_{eq} may be approximated by an average fixed value. Also, if the variation in resistance can be approximated by a known function, say, linear, quadratic, and so on, an equivalent resistance can be derived by using a simple integration. For an average R_{eq}, head noise can be calculated from equation (8.18).

The inductive head equivalent circuit is also applicable for the MR head except the MR head is represented by a single-turn head. Its inductance is just the inductance of the leads. Typical values of parameters for MIG, two versions of thin film heads, and the MR head are shown in Table 5.1. The resistance of a 5-μm-long, 30-nm-thick, 2-μm-high MR stripe is about 20 Ω. Head noise is calculated using Equation (8.18) as 0.58 nV/$\sqrt{\text{Hz}}$.

8.21 HEAD PREAMPLIFIER NOISE

In equation (8.17), the second term is the noise due to input preamplifier. The head signal is under 1 mV, and its amplification by the front end of the read electronics requires special care. Low-noise, wide-band preamplifiers are designed as a part of an LSI circuit.

Figure 8.31 is the schematic of a differential preamplifier commonly used to amplify a head signal. Once the preamplifier amplifies the signal to between 20 and 100 times the head output, later stages of amplification and detection do not contribute significantly to the overall signal-to-noise ratio of the system and can be neglected. A differential amplifier is used as an input stage instead of a conventional single transistor in order to eliminate common mode noises, including voltage line transients and disturbances. The common mode noises and disturbances will swing (vary) both outputs of the differential amplifier; hence, the differential voltage remains unaffected by the extraneous perturbations, and the output will represent the input more accurately. The noise voltage E_{np} is a function of base resistance and gain β of the transistor. Wide-area transistors with narrow base widths are used to reduce the base resistance of the transistor with high gain. The noise voltage of the amplifier can be measured by shorting the input and observing the output, which is amplifier internal noise times the gain. There are three broad classifications of noise sources found in a transistor:

1. Flicker (or $1/f$) noise
2. Thermal noise
3. Shot noise

Flicker noise is a low-frequency phenomenon, and in wide-band applications it can be limited to very low frequencies. It is neglected for amplifiers for recording

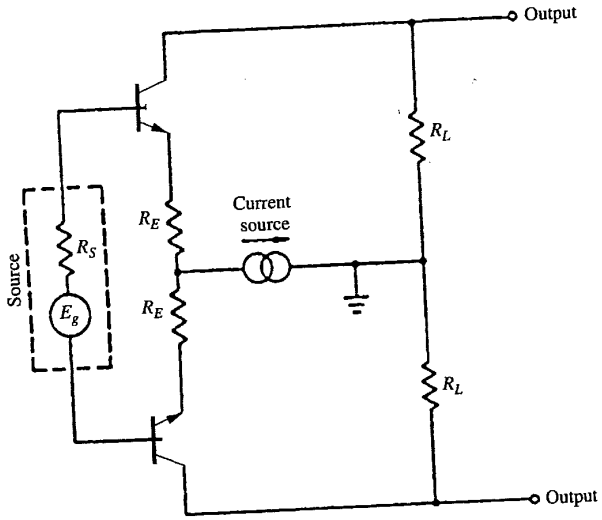

Figure 8.31 Schematic of a differential preamplifier.

applications. Thermal noise is largely due to the base resistance of a transistor and is generally quoted in amplifier specifications. Shot noise is due to current flow in the base-to-emitter diode of the transistor. Thermal noise is calculated using equation (8.18) once the resistance value is specified. The shot noise can be important for high-impedance (ferrite and MIG) heads.

Reference [9] analyzes these topics in more detail. It is a common practice to match the head and preamplifier noises for compromise between minimization of the total noise and adequate signal bandwidth. Preamplifiers are designed to provide input noise range between 0.5 and $2nV/\sqrt{Hz}$. We shall use 1.0 nV/$\sqrt{\text{Hz}}$ as an example for the discussion of signal and noise.

8.22 THIN FILM MEDIUM NOISE

Medium noise from the view of medium design is discussed in Section 7.4. Here we shall describe the characteristics of film medium noise and an experimental procedure to measure it. The noise in thin film medium originates in the transitions in which magnetizations change directions. The DC-erased noise of film medium is negligibly small. Since the noise originates in the transitions, measurement of the noise requires presence of a recorded signal. Also, because the noise source is in transitions that can be located on a disk track, it is possible to separate the thermal noise of the head and preamplifier by time averaging. Simple and practical methods for separating electronic and media noises are illustrated in Figure 8.32 [10].

The output of the head amplifier is connected to a spectrum analyzer. First, the head noise is measured when the head is lifted away from the disk. The noise spec-

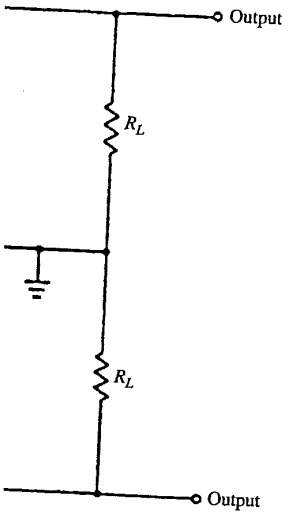

fferential preamplifier.

ıe base resistance of a transistor and is
hot noise is due to current flow in the
ıal noise is calculated using equation
The shot noise can be important for

ore detail. It is a common practice to
ımpromise between minimization of
. Preamplifiers are designed to pro-
Hz. We shall use 1.0 nV/$\sqrt{\text{Hz}}$ as an

n is discussed in Section 7.4. Here
ıedium noise and an experimental
ıedium originates in the transitions
DC-erased noise of film medium is
he transitions, measurement of the
lso, because the noise source is in
is possible to separate the thermal
ing. Simple and practical methods
ustrated in Figure 8.32 [10].
d to a spectrum analyzer. First, the
vay from the disk. The noise spec-

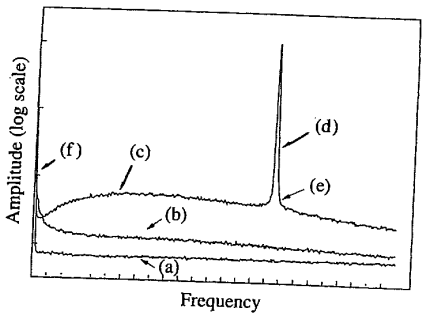

Figure 8.32 Measurement of media noise [10].

trum [curve (a)] is measured in this condition. This is only head and preamplifier electronic noise. Curve (b) is the measured noise from DC-erased media. Next a single-frequency sinusoidal signal is recorded on the disk track and a total recorded spectra is measured [curve (c)]. Curve (d) indicates the recorded single sinusoidal frequency signal. The difference between smoothed curve (c) (after eliminating single-peak frequency and DC-peak response at $f = 0$) and electronic noise spectra gives the medium noise spectrum. For most applications, a straight-line noise value is averaged for the medium, and the noise amplitude is given in nanovolts per square root of hertz. Reference [10] also discusses corrections needed in the use of the spectrum analyzer and alternative time domain measurements.

8.23 SIGNAL-TO-NOISE RATIO AND ON-TRACK ERROR RATES

A formalism to relate measurements of intersymbol interference, signal and component noise sources to error rate for a peak detection channel has been described [11]. It is desirable to have analytical equations relating these quantities in a closed form. It is difficult to obtain a single general equation to relate these parameters. In this section, several equations are discussed which give insight into the quantitative relationships among these variables. An understanding of these interactions could be helpful in formulating analytical or computer modeling of channel error rates. The track density and more generalized modeling of error rates in a system are discussed in Chapter 9.

With noise voltages either computed or measured, total noise voltage for the three factors discussed in the last section is calculated using equation (8.17). Let the zero-to-peak voltage of the signal to be detected be E_{0p}. Then the traditional definition of the signal-to-noise ratio in recording is

$$\text{SNR} = \frac{S}{N} = \frac{E_{0p}}{E_{nt}}; \quad \left(\frac{S}{N}\right)_{dB} = 20\log_{10}\left(\frac{E_{0p}}{E_{nt}}\right) \tag{8.20}$$

Note that the average noise voltage of random sources is zero. Here, E_{nt} is the RMS value of the combined noises and standard deviation of the error function or the Gaussian distribution. Figure 8.30 shows how the zero crossing location of the signal gets shifted by time t_n due to random noise. The following discussion considers the peak shift in signal due to only random noises. The standard deviation of distribution of variable t_n is defined as σ_n. It is assumed that σ_n is proportional to E_{nt}, that is, $\sigma_n = E_{nt}/k$; the distribution of t_n is expressed as

$$P(t_n) = \frac{1}{\sqrt{2\pi}\sigma_n} e^{-1/2(t_n/\sigma_n)^2} \tag{8.21}$$

Error occurs if t_n exceeds half the window ($T_w/2$) on either side of the window center. This is described as

$$P(E) = \int_{-\infty}^{-T_w/2} p(t_n)\,dt_n + \int_{T_w/2}^{\infty} p(t_n)\,dt_n = 2\int_{T_w/2}^{\infty} p(t_n)\,dt_n \tag{8.22}$$

The function erfc(z), which is equal to 1 − erf(z), is defined as

$$\text{erfc}(z) = \frac{2}{\sqrt{\pi}} \int_z^{\infty} e^{-u^2}\,du \tag{8.23}$$

Changing the variable $u = (t_n)/(\sqrt{2}\sigma_n)$, and substituting equation (8.22) in (8.23), the probability of error is obtained:

$$P(E) = \text{erfc}\left(\frac{T_w}{2\sqrt{2}\sigma_n}\right) \tag{8.24}$$

Substituting $\sigma_n = E_{nt}/k$ and E_{nt} from equation (8.20), equation (8.24) is rewritten as

$$P(E) = \text{erfc}\left(\frac{kT_w\text{SNR}}{2\sqrt{2}E_{0p}}\right) \tag{8.25}$$

The equation thus gives the probability of an error, or the bit error rate, in terms of SNR, the peak voltage for a given size of time window. Assuming the Lorentzian signal pulse and other simplifications, the following equation is obtained [12]:

$$P(E) = \text{erfc}\left(\frac{\sqrt{2}T_w\text{SNR}}{P_{50}}\right) \tag{8.26}$$

If the error rate is specified as 10^{10}, or 1 error in 10^{10} bits read, the corresponding T_w can be obtained from the above equation using a look-up table of erfc functions. This is the minimum time window required to satisfy the error rate specification for given SNR and P_{50}. The resultant equation is [12, 13]

m sources is zero. Here, E_{nt} is the RMS
l deviation of the error function or the
)w the zero crossing location of the sig-
ise. The following discussion considers
noises. The standard deviation of dis-
assumed that σ_n is proportional to E_{nt},
:xpressed as

$$e^{-1/2(t_n/\sigma_n)^2} \tag{8.21}$$

$(T_w/2)$ on either side of the window

$$(t_n)\,dt_n = 2\int_{T_w/2}^{\infty} p(t_n)\,dt_n \tag{8.22}$$

f(z), is defined as

$$e^{-u^2}du \tag{8.23}$$

ubstituting equation (8.22) in (8.23),

$$\frac{T_w}{\sqrt{2}\sigma_n}\Bigg) \tag{8.24}$$

(8.20), equation (8.24) is rewritten

$$\frac{\text{SNR}}{2E_{0p}}\Bigg) \tag{8.25}$$

ror, or the bit error rate, in terms of
window. Assuming the Lorentzian
ving equation is obtained [12]:

$$\frac{\text{SNR}}{50}\Bigg) \tag{8.26}$$

10^{10} bits read, the corresponding
g a look-up table of erfc functions.
isfy the error rate specification for
2, 13]

$$T_w \geq \frac{4.573P_{50}}{\sqrt{2}\text{SNR}} \tag{8.27}$$

The equation indicates that a large SNR and small P_{50} or slimmer pulse are desirable to keep the noise-related window narrow. Note that only random noises are included in the SNR in this equation. Figure 8.29 shows that there are other sources of (nonrandom) noises that contribute to peak shifts. The total window required to meet the bit error rate objective would be significantly wider than that indicated by the equation. In Section 9.13, following the discussion of off-track and adjacent track noises, the window margin integration procedure for the head-disk system is described.

REFERENCES

[1] A. M. Patel, "Signal and Error-Control Coding," in *Magnetic Recording Handbook,* C. Denis Mee and Eric D. Daniel, eds., McGraw-Hill, New York, 1990.

[2] P. H. Siegel, "Recording Codes for Digital Magnetic Storage," *IEEE Trans. Magn.,* MAG-21 (1985), p. 1344.

[3] R. L. Comstock and M. L. Workman, "Data Storage on Rigid Disks," in *Magnetic Recording Handbook,* C. Denis Mee and Eric D. Daniel, eds., McGraw-Hill, New York, 1990, p. 655.

[4] T. Kameyama, S. Takanami, and R. Arai, "Improvement of Recording Density by Means of Cosine Equalizer," *IEEE Trans. Magn.,* MAG-12 (1976), p. 746.

[5] J. G. Proakis, *Digital Communications,* McGraw-Hill, New York, 1983.

[6] A. M. Patel, "A New Digital Signal Processing Channel for Data Storage Products," *IEEE Trans. Magn.,* MAG-27 (1991), p. 4579.

[7] R. F. Hoyt and H. Sussner, "Precise Side Writing Measurements Using a Single Recording Head," *IEEE Trans. Magn.,* MAG-20 (1984), p. 909.

[8] R. L. Comstock and M. L. Williams, "Frequency Response in Digital Magnetic Recording," *IEEE Trans. Magn.,* MAG-9 (1973), p. 342.

[9] K. B. Klaassen, "Magnetic Recording Channel Front-Ends," *IEEE Trans. Magn.,* MAG-27 (1991), p. 4503.

[10] L. L. Nunnelley, "Practical Noise Measurements," in *Noise in Digital Magnetic Recording,* T. C. Arnoldussen and L. L. Nunnelley, eds., World Scientific, Singapore, 1992, p. 257.

[11] E. R. Katz and T. G. Campbell, "Effect of Bit Shift Distribution on Error Rate in Magnetic Recording," *IEEE Trans. Magn.,* MAG-15 (1979), p. 1050.

[12] A. S. Hoagland and J. E. Monson, *Digital Magnetic Recording,* John Wiley & Sons, New York, 1991, p. 213.

[13] E. Williams, in *Noise in Digital Magnetic Recording,* T. C. Arnoldussen and L. L. Nunnelley, eds., World Scientific, Singapore, 1992, p. 233.